FIRE SPREAD PREDICTION ACROSS FUEL TYPES: ANNUAL PROJECT REPORT 2018-19

Mahmood Rashid[1], Duncan Sutherland[1,2], Khalid Moinuddin[1]
Centre for Environmental Safety and Risk Engineering, Victoria University, VIC
School of Physical, Environmental and Mathematical Sciences, UNSW, Canberra, ACT

Version	Release history	Date
1.0	Initial release of document	20/06/2019

Disclaimer:
Victoria University and the Bushfire and Natural Hazards CRC advise that the information contained in this publication comprises general statements based on scientific research. The reader is advised and needs to be aware that such information may be incomplete or unable to be used in any specific situation. No reliance or actions must therefore be made on that information without seeking prior expert professional, scientific and technical advice. To the extent permitted by law, Victoria University and the Bushfire and Natural Hazards CRC (including its employees and consultants) exclude all liability to any person for any consequences, including but not limited to all losses, damages, costs, expenses and any other compensation, arising directly or indirectly from using this publication (in part or in whole) and any information or material contained in it.

TABLE OF CONTENTS

ACKNOWLEDGMENTS

We acknowledge the Ancestors, Elders and families of the Boonwurrung, Waddawurrung and Woiwurrung language group of the Kulin who are the traditional owners of University land. As we share our own knowledge practices within the University may we pay respect to the deep knowledge embedded within the Aboriginal community and their ownership of Country.

We acknowledge that the land on which we meet is a place of age old ceremonies of celebration, initiation and renewal and that the Kulin people's living culture has a unique role in the life of this region.

EXECUTIVE SUMMARY

Prediction of the rate of spread and intensity of bushfires is crucial for the emergency and disaster management organisations for operational planning and to deploy their resources. Currently, simplified operational models are used as the prediction can be obtained on time scales commensurate with those required by emergency managers. Our aim is to refine these non-physics-based operational tools so that they can predict fire behaviour under a wide range of localised topographic and weather conditions and they are able to account for a range of inhomogeneity, slope, and thermal instability within vegetation and over the terrain. Furthermore, a more physically-motivated firebrand model needs to be included in operational models to predict firebrand landing and increased rate of fire spread (RoS).

In last few years, we have numerically tested and established a reliable physics-based model that is based on basic fire dynamics theory and corresponding differential equations to simulate bushfire scenarios. We now embark upon utilization of our research as well as extending parametric study using the physics-based model. The the following aspects have been the highlights of our endeavour:

- The effect of a tree canopy on the near surface wind speed with a view to modelling the wind reduction factor (WRF) due to the canopy. The wind reduction factor is used in operational fire prediction models such as the McArthur model, to account for the reduction in wind velocity due to a tree canopy. We developed understanding of subcanopy wind flow through homogenous, longitudinally heterogeneous and vertically heterogeneous forest canopies. We are now attempting to simulate flow through canopies with varying atmospheric stability and homogenous canopy over a hill. We have also began implementation of WRF based on our research into an operational platform (SPARK of CSIRO's Data61).
- Simulations rate of grassfire as functions of wind, grassheight, slope, intial windfield etc with view to improve Australian Standard AS3959. Foundations of rigourous simulation has been laid through a number of journal paper publications and we are now exploring various parametric studies. In one such study, we evaluated heat load from incoming grassfire on structures in relation to AS3959.
- Transport of non-burning firebrand (three particle shapes, cubical, cylindrical, and disc shaped particles, representing idealised firebrands) and their landing distribution with view to develop operational models of ember attack for quantification in AS3959. We have extended the simulation work to study the transport of ember particles across realistic forest edges. The results show that lower sphericity of the firebrand can increase lateral dispersion.
- Reducing the spin-up time for the physics-based model and initialise the wind fields for faster and efficient fire predictions. This is attempted by using Windninja which is a computer program to compute spatially varying wind fields over a complex terrain. We have successfully mapped the terrain modified wind fields generated by Windninja to the physics-based model using the penalization method. We are also able to implement gusting behaviour in the physics-based model.

Overall we have achieved our goal of obtaining greater insight into bushfire physics and we are now utilizing those insights to parameterize various phenomenon for operational models.

END USER STATEMENT

END USER STATEMENT

INTRODUCTION

With the fast increase of computational power, simulations of bushfire phenomenon using physics-based models in greater field-scale are becoming possible. By "physics-based model" it is meant that all modes of heat transfer (conduction, convection, radiation) present in both the fire-fuel and the fire-atmosphere interactions; production and transport of firebrand; and ignition, gasification and combustion of solid fuels are modelled. Physics-based modelling can be used to bridge the gap between the empirical models that are based on observation and scientific theories. Empirical models are computationally cheap to implement and require only few parameters which make them user friendly. However, these models are only truly valid in the range of conditions in which these were developed (often in benign conditions) and are highly dependent on the conditions in which the source data were obtained for model development. As Sullivan [1] remarked, empirical models are based on observations, and not on theory. Studies show with empirical models, an estimation error, in the rate of spread, can be around 40-60% [2]. Physics-based models can be used for improved parameterization of empirical models. Many parameters used in empirical models are determined by fitting experimental rate of spread. It is important to understand the science behind those choice of parametric values and even better to develop more scientific values which will improve predictions.

To address existing gaps in the mathematical/computational modelling of bushfire dynamics, we focus on three distinct areas (a) subcanopy wind flow, (b) grassfire propagation and (c) firebrand transport.

The rate at which fires spread is strongly dependent on the wind speed. This is true for fire over open grassland as well as through and over forests. The velocity profile of the wind within forests is quite different from that over open ground. The dependence of wind speed reduction on forest canopy density is being explored. By comparing wind profiles entering and leaving the canopy we are developing a tool to determine an appropriate Wind Reduction Factor (WRF). In last few years, we developed understanding of subcanopy wind flow through homogenous, longitudinally heterogeneous and vertically heterogeneous forest canopies. We are now attempting to simulate flow through canopies with varying atmospheric stability and homogenous canopy over a hill. We have also began implementing WRF based on our research into an operational platform.

Simulations rate of grassfire as functions of wind, grassheight, slope, intiail windfield etc have been major highlights of our studies. Foundations of rigourous simulation has been laid through a number of journal paper publications and we are now exploring various parametric studies. In one such study, we evaluated heat load from incoming grassfire on structures in relation to Australian Standard AS3959 [3] which was developed to specify necessary structural changes for the structures located at Bushfire Prone Areas (BPA). We also endeavour to reduce spin-up time for grassfire modelling by initialising the wind fields from reduced models for faster and efficient fire predictions.

The rate of spread of bushfires is often dominated by firebrands being conveyed ahead of the firefront. We have improved and validated physics-based models capability to accurately simulate how firebrands disperse. This is being further utilised to study the behaviour of firebrand transport under different weather, vegetation and terrain conditions. We envisage formulating a parameterisation of firebrand transport and landing distribution which can be used with operational models as well quantification of firebrand flux on structures to be included in AS3959.

The key motivation of our work is to improve bushfire modelling so that risks and losses can be reduced. Results from above areas will be utilised to develop application tools for fire behaviour analysts/regulators.

//

THE PROJECT – ACHIEVEMENTS

MODELLING WIND FLOW AND SURFACE FIRE THROUGH CANOPIES

Physics-based modelling of subcanopy wind flow is one of the three streams of our research. This stream is aimed at developing an operational model for wind reduction factor (WRF) due to the canopy. The wind reduction factor is used in operational fire prediction models such as the McArthur model, to account for the reduction in wind velocity due to a tree canopy. In last few years, we developed understanding of subcanopy wind flow through homogenous, longitudinally heterogeneous and vertically heterogeneous forest canopies. We are now attempting to simulate flow through canopies with varying atmospheric stability and homogenous canopy over a hill.

Preliminary simulation of flows through canopies with varying atmospheric stability

During the night, the ground is cooler than the atmosphere while the ground is hotter during the day. Due to this temperature difference, the mean wind speed profile observed in the atmospheric surface layer (ASL) takes different form than an ASL in neutral (no temperature difference) conditions. An atmosphere can be considered stable, when the ground is cooler (in the later part of the night extending to the early morning) and an atmosphere can be considered unstable, when the ground is hotter resulting in lifting of air (in the middle part of the day to dusk time). However, a temperature difference may occur any time between the atmosphere and ground depending on weather conditions. An idealised ASL is a boundary layer between a rough ground surface and atmosphere. However, having a closer look at the ground surface features (such as forest or urban canopy), we may find that ASL may take different forms. Knowledge of such forest canopy-ASL interaction is of great interest in many applications, such as, climate change, greenhouse gases between forests and atmosphere, wind damage and wind throw at forest edges, the spreading of wildfires and dispersion of pollen and pollutants [4].
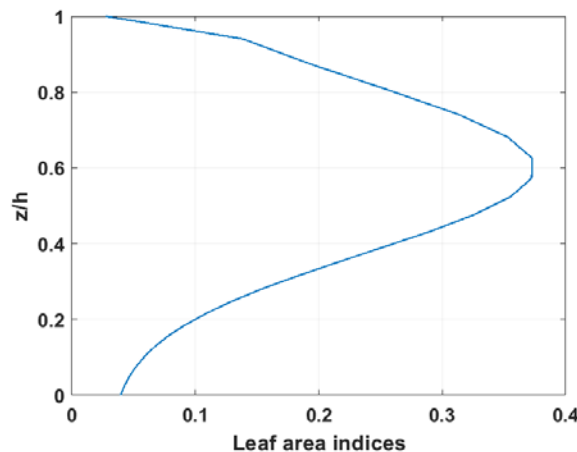

FIGURE 1: LAD PROFILE OF SCOTS PINE TREE

Large eddy simulation (LES) is performed for flows through forest canopy applying various atmospheric stability conditions. The canopy is modelled as a horizontally homogenous region of aerodynamic drag with a leaf-area density (LAD) profile approximating the profile of a Scots pine tree. The LAD profile is shown in Figure 1, which is produced based on the method following Sutherland et al. [5].

Varying atmospheric stability is incorporated into the simulation by applying varying heat flux in two different ways:

(i) prescribing surface heat flux using Monin-Obukhov similarity functions and,

(ii) applying canopy heat flux where heat from the canopy is modelled as distributed volume heat source.

For the first category of simulations, atmospheric temperature are used as an input parameter and then surface heat flux is modelled by Monin-Obukhov similarity functions. A wind profile is generated with an introduction of suggested Obukhov lengths in the physics-based model Fire Dynamics Simulator (FDS) [6], which is derived from Monin-Obukhov similarity functions for momentum and heat. According to these similarity functions, mean velocity and mean temperature are varied with height (z) (without the presence of any forest canopy) as following equations:

$$u(z) = \frac{u_*}{k}\left[ln\left(\frac{z}{z_0}\right) - \psi_M\left(\frac{z}{L}\right)\right] \tag{1}$$

$$\theta(z) = \theta_0 + \frac{\theta_*}{k}\left[ln\left(\frac{z}{z_0}\right) - \psi_H\left(\frac{z}{L}\right)\right] \tag{2}$$

where, z_0 is the aerodynamic roughness length (≈ 0.02), k is Von Karman's constant (≈ 0.41), θ_0 is ground level potential temperature and Monin Obukhov length, L, is defined by

$$L = \frac{u_*^2 \theta_0}{\theta_* g k} \tag{3}$$

In Eq (3), g is the acceleration of gravity, θ_* is the scaling potential temperature defined as :

$$\theta_* = T\left(\frac{p_0}{p}\right)^{R/(/W_{air}C_p)} \tag{4}$$

where p_0 is typically 1000 mbar and $R/(/W_{air}C_p) \approx 0.286$, and u_* is the friction velocity defined as:

$$u_* = \frac{k\, u_{ref}}{ln\left(\frac{z_{ref}}{z_0}\right)} \tag{5}$$

where u_{ref} velocity is taken at a reference height of z_{ref}. Additionally, the similarity functions, ψ_M and ψ_H are implemented according to proposed Dyer's model [7].

For the first category, the simulation of five classes of stabilities are studied as shown in Table 1. These cases are categorized in terms of Obukhov length which enforces ground heat flux in the simulations.

TABLE 1: CASES FOR SURFACE HEAT FLUX MODELS (CATEGORY 1)

Stability type	Obukhov length, L	Physical meaning
stable	350	Surface is cooler than atmosphere
unstable	-350	Surface is hotter than atmosphere
neutral	1000000	Same temperature as surface and atmosphere
very stable	100	Surface is more cooler than stable case
very unstable	-100	Surface is more hotter than unstable case

The simulation domain is set up with a rectangular domain of (*30h x 15h x 5h*) as shown in Figure 2. *h* is the canopy height which is taken as 20 m. Meshing is done in an FDS coordinate system with *x, y* and *z* relate to the streamwise, lateral and vertical directions, respectively with a grid number of (*120, 60, 50*) cells. A grid stretching is applied in the vertical direction following FDS polynomial mesh leading to a resolution of approximately 0.25 m at bottom of the domain. Periodic boundary conditions are applied in both the streamwise and the lateral directions, while a symmetry boundary condition is applied at the top of the domain. A horizontally homogenous pine forest tree is integrated in *xy* plane with the canopy in the entire domain. The bottom of the domain is treated as a ground with an ambient temperature of 20^0C.
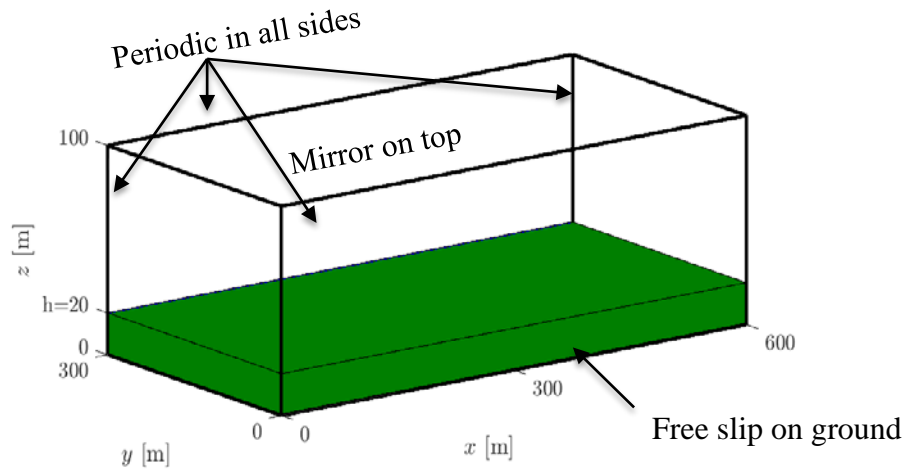

FIGURE 2: SIMULATION DOMAIN: GREEN COLOUR IS THE HOMOGENEOUS CANOPY AND BOUNDARY CONDITIONS ARE LABELLED BY ARROW SIGN.

The streamwise horizontal mean velocity variation with height is shown in 3(a) for different stability cases for comparison purposes. First, the velocity profiles seem realistic in the context of development of wind profile with an inflection point in dense canopy region and subsequent generation of profile according to different stability definitions applied with the help of Monin-Obukhov length. It seems realistic that the stable and unstable profiles are showing shifted towards right to neutral velocity profile indicating wind dominated flow. Moreover, unstable and very unstable profiles become more vertical
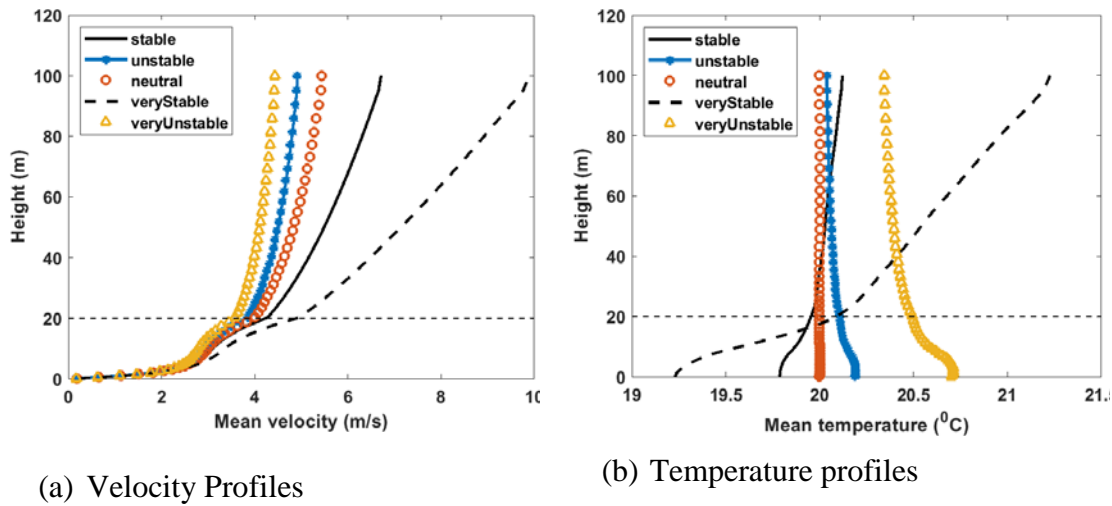
(a) Velocity Profiles

(b) Temperature profiles

FIGURE 3: RESULTS FROM SURFACE HEAT FLUX PRESCRIPTION

with a clear evidence of buoyant contribution of turbulent kinetic energy comparing to neutral, stable and very stable cases. Heated ground contributes to this buoyancy. It may be anticipated that with very stable scenario, a sub-canopy or above-canopy fire can spread quickly than other scenarios, as the wind can lean the flame more close to unburnt fuel ahead and heat them up more quickly via radiation and convection.

Mean temperature profiles are also shown in Figure 3(a) for all stability classes. The temperature profile of a neutral case is showing no change in temperature as expected in neutral situation. For the very stable case, there is a significant increase of atmospheric temperature compared to ground as the thermal stratification (in air) causing temperature to rise in atmosphere. However, for unstable cases, there is a decrease of temperature in atmosphere and higher temperature on ground causing negative temperature gradient in unstable situation as expected. Overall, there is a decrease in temperature in all unstable cases while temperature has increased in all stable cases in atmosphere compared to ground that are expected.

TABLE 2: CANOPY HEAT FLUX MODELS (CATEGORY 2)

Stability	Flux condition	Physical meaning
stable	Negative volumetric heat flux	Surface is cooler than atmosphere
unstable	Positive volumetric heat flux	Surface is hotter than atmosphere
neutral	No heat flux added	Same temperature as surface and atmosphere

For the second category, three cases are simulated as shown in Table 2, where we applied volumetric heat flux as an input data. The volumetric heat flux is varied from canopy top to downward as shown in Figure 4 for the stable and unstable cases. We applied maximum heat flux at canopy top to a minimum at 10 m down in dense canopy region towards ground following the heat source model done by Nebenfuhr et al [4] and Shaw et al. [8]. Mean velocity and temperature profiles are not prescribed using Eqs (1-5). Rather, a pressure driven wind profile is generated applying a force vector in the streamwise direction to develop a wind profile with temperature stratification due to applied heat

flux. The neutral case is set up with same pressure driven wind profile but without any input of heat flux.

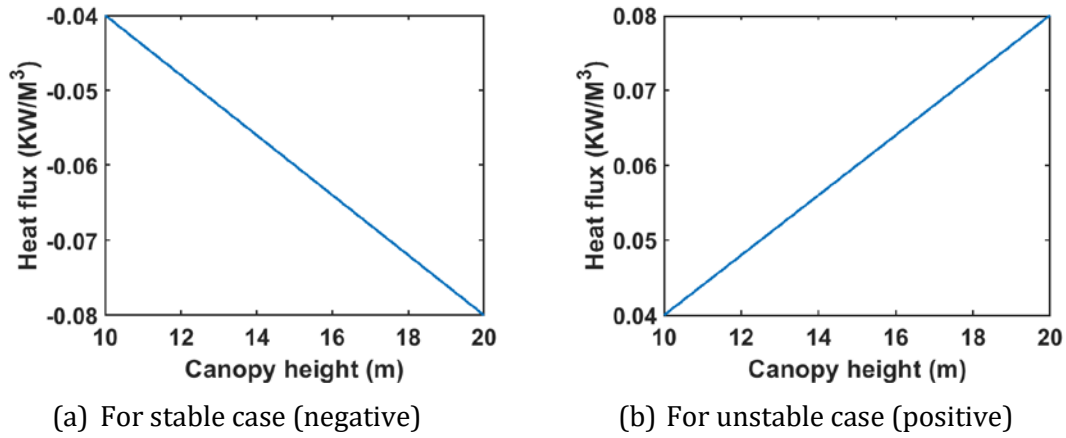(a) For stable case (negative) (b) For unstable case (positive)

FIGURE 4: APPLIED THERMAL STRATIFICATION (LINEAR HEAT FLUX) WITHIN CANOPY FROM CANOPY TOP TO 10M DOWN

The mean horizontal velocity variation with height is shown in Figure 5(a) for the stable, unstable and neutral cases obtained using the canopy heat flux model. Comparing to our previous surface heat flux classes, the mean velocity profiles are showing similar trend in canopy heat flux models with due inflection point and subsequent development of wind profile. The stable and unstable classes are showing increasing and decreasing velocity compared to the neutral class; respectively following similar trend that we have seen in the surface heat flux models (category 1).

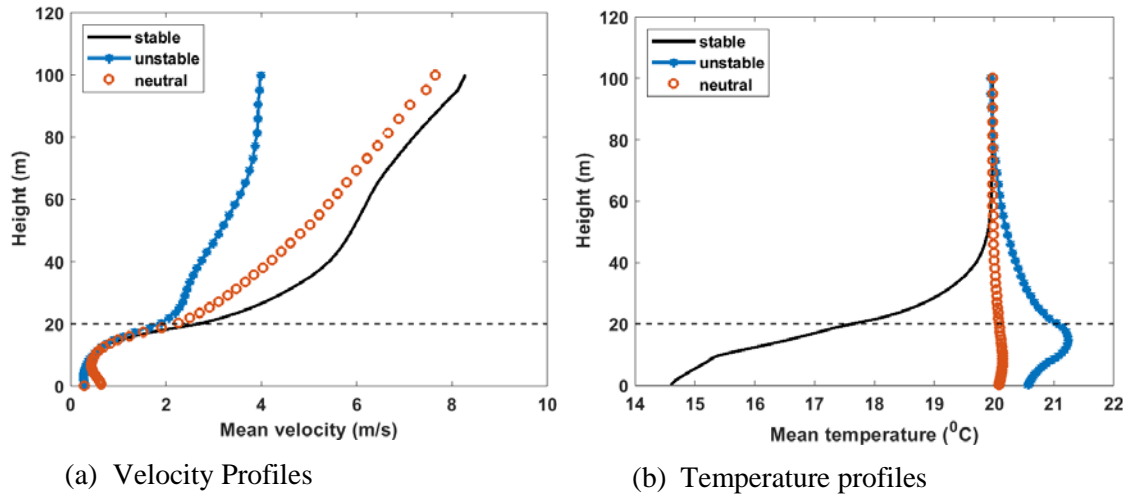(a) Velocity Profiles (b) Temperature profiles

FIGURE 5: RESULTS FROM CANOPY FLUX MODEL

The mean temperature profiles obtained using the canopy heat flux model are shown in Figure 5 (b), which shows similar trend as we have seen in the surface heat flux model. The increase and decrease of mean temperature in atmosphere at stable and unstable classes compared to neutral class; respectively clearly showing the trend as expected. However, for the neutral case, although a little disagreement in dense canopy region is observed but mean temperature remains unchanged as expected.

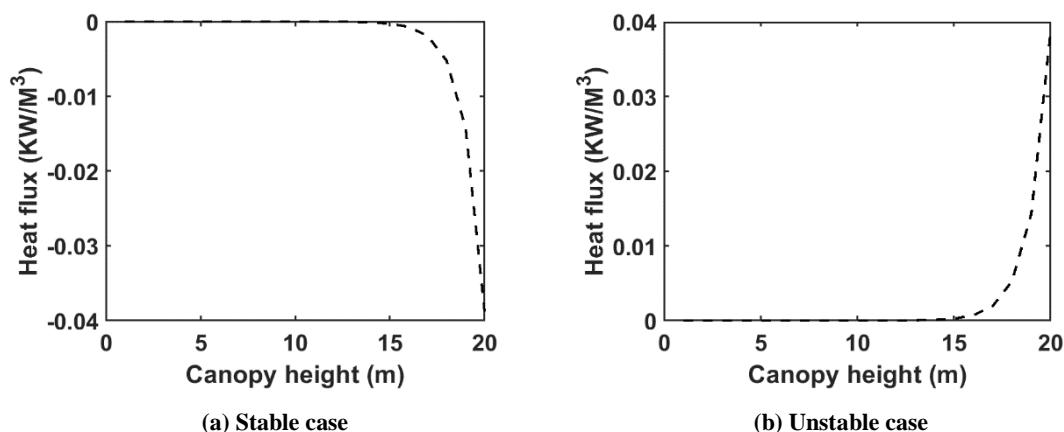|	
(a) Stable case	**(b) Unstable case**

FIGURE 6: THERMAL STRATIFICATION TO BE APPLIED FOR MODEL VALIDATION

The next set of future simulations will use a more realistic exponentially decreasing heat flux profile from the canopy top to the bottom that depends upon the LAD. The exponential decreasing flux profile is shown in Figure 6 for the stable and unstable classes. The aim will be to validate the simulation results against existing data in the literature. In Nebenfuhr et al. [4], a heat source was applied as a source term in a temperature transport equation with varying heat flux in the domain from canopy top to downward. Subsequently, Nebenfuhr compare their simulation results to experimental observations. FDS, however, uses the ideal gas equation to obtain temperature field and instead includes heating terms in the velocity divergence equation. Because of the different approaches, the simulation results from FDS need to be carefully compared to other simulations and experimental data to ensure they are correct. Once the validation is done successfully, this study can be extended for fire propagation cases in future.

Work on implementation of WRF obtained from Physics-based model into operational platform SPARK of CSIRO Data61

As our modelling work is maturing, we are aiming to implement our research into CSIRO's operational platform SPARK. After performing feasibility study we have come up with three different frameworks to implement physics-based WRF for the end users (See Figure 7). We found option 2 as the most suitable among the available options.
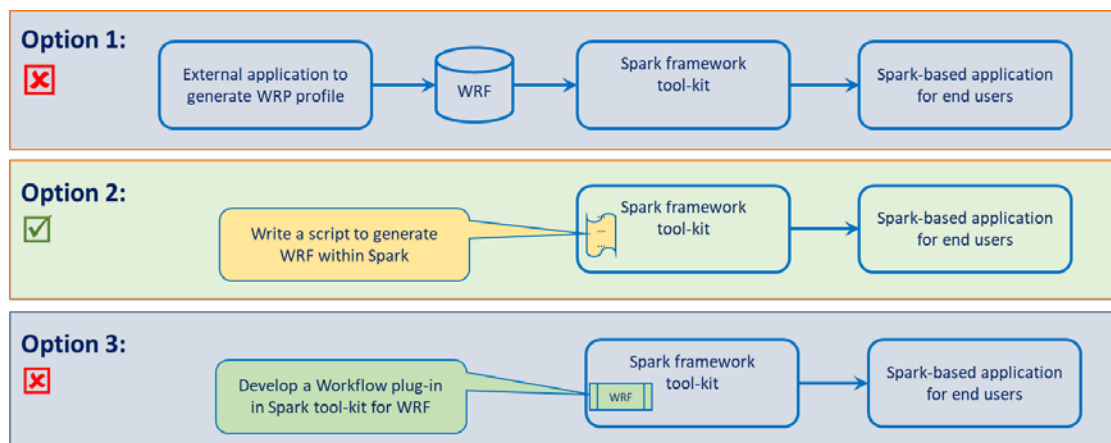

FIGURE 7: THREE DIFFERENT OPTIONS OF THE PROPOSED UTILISATION FRAMEWORK. WE ARE GOING TO PROCEED WITH OPTION 2.
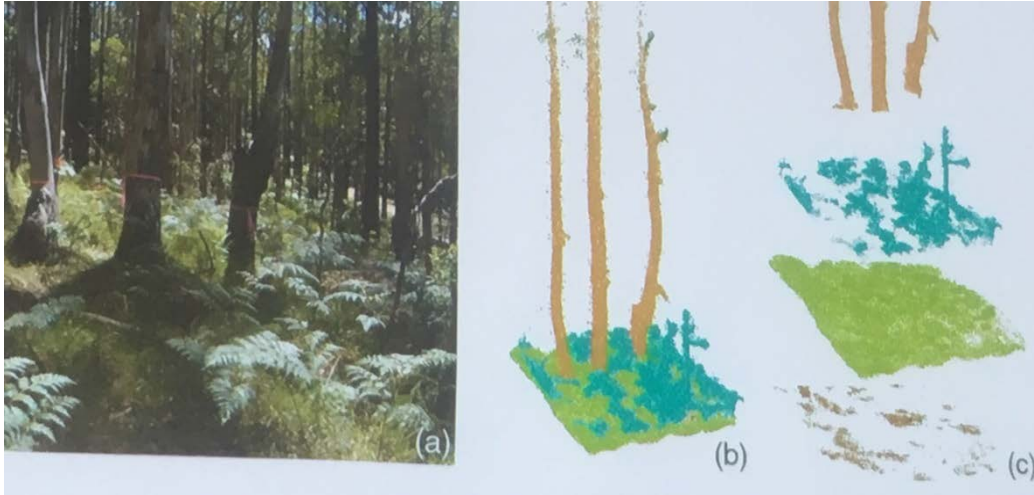
FIGURE 8: RECONSTRUCTION OF FUEL STRUCTURE AND QUANTIFICATION USING LIDAR (COURTESY: DR MARTHA YEBRA, AUSTRALIAN NATIONAL UNIVERSITY). (A) ACTUAL FOREST, (B) COMBINED RECONSTRUCTION AND (C) SEPARATION OF EACH KIND OF FUEL STRATA. LAD CAN BE DERIVED FROM (B).

Option 2 involves calculation of the WRF dynamically in a Spark script based on some mathematical model (e.g. between wind strength and vegetation type). We are considering Inoue-Harman-Finnigan model [9, 10] and the Mossman et al. [11] model. However, it is to be noted that both models are very similar. The original model of Inoue is developed from a momentum-balance approach and is used to determine the sub-canopy wind profiles deep within a canopy. The model of Harman and Finnigan [10] extends the original model of Inoue to blend neatly with a roughness sub-layer and logarithmic layer above the canopy. The model was constructed from an established model of sub-canopy and above canopy wind profile due to Harman and Finnigan [10], and from a logarithmic open wind speed model. The models were matched at some assumed blending height, and the wind reduction factor was computed as the ratio of the two models.
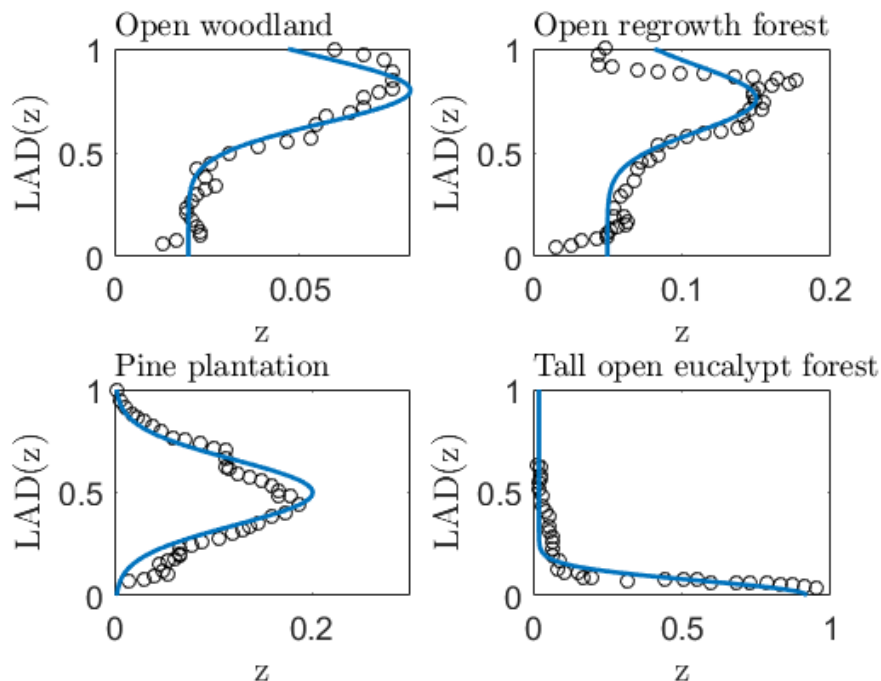

FIGURE 9. PROFILES OF LAD MEASURED BY [12] FOR FOUR DIFFERENT FOREST TYPES. BLUE LINES REPRESENT MATHEMATICAL EXPRESSIONS.

These models are based on leaf area index (LAI) which is relatively easily available from [13]. It is to be noted that LAI is only provides a dimensionless measure (with single value) of vegetation per unit of ground area. Basically treats all leaves as flat, one dimensional sheets, and measure the amount of green relative to an area on the ground. In future, the WRF model will likely become more complicated and depend on leaf area density (LAD), flame height and intensity, so we are considering laying the foundations for those ideas now.

LAD describes vertical and horizontal structures of tree canopies (vegetation per unit volume of tree canopy). Figure 8 demonstrates how fuel structure of an actual forest can be collected using LiDAR and then three-dimensionally reconstructed and quantified. LAD can be derived from Figure 8(b) and will need to be put in a two-dimensional mathematical framework.

Profiles of LAD measured by [12] for four different forest types are presented in Figure 9. These profiles can be idealised mathematically and mathematical idealisations are presented with blue lines. LAD data as shown in Figure 9 may be available for ACT and some part of NSW.

Option 1 is not totally discarded which involves reading a pre-prepared map of the WRF based on an external calculation into Spark. However, this needs a long term project to first to obtain LAD for a particular jurisdiction or Australia-wide. Once the map of LAD is available, interface behaviour at the junction of course & sparse canopy will also need to be included f the operational models.

MODELLING OF GRASS FIRE

Effect of grass height on the rate of grassfire spread

Our first grassfire modelling paper is published in prestigious International Journal of Wildland Fire [14]. In this paper, a systematic approach to grassfire modelling using a physics-based model through the establishment of the atmospheric boundary layer and grid convergence is presented. A successful reference case (grass fire experiment conducted by Cheney et al [15]) simulation is followed by a study of grassfire cases that tests the effects of wind speed and grass height, independently. In this study, the rate-of-spread (RoS) obtained from the physics-based model is found to be linear with wind speed in the parameter range considered. When wind speed is varied, the physics-based model predicts faster RoS than the Mk III and V (McArthur) model (Noble et al [16], but slower than the CSIRO model (Cheney et al. [17]). This is shown in Figure 10.

When the grass height is varied, keeping the bulk density constant, the fire front changes from a boundary layer flame mode to plume flame mode as the grass height increases. Once the fires are in plume mode, a higher grass height results in a larger heat release rate of the fire but a slower RoS. The result is presented in Figure 11.

This study is conducted in collaboration with Dr William (Ruddy) Mell at US Forest Services who is the developer of physics-based model for Wildfire used for this study. The study has become the foundation of our further grassfire simulation studies.
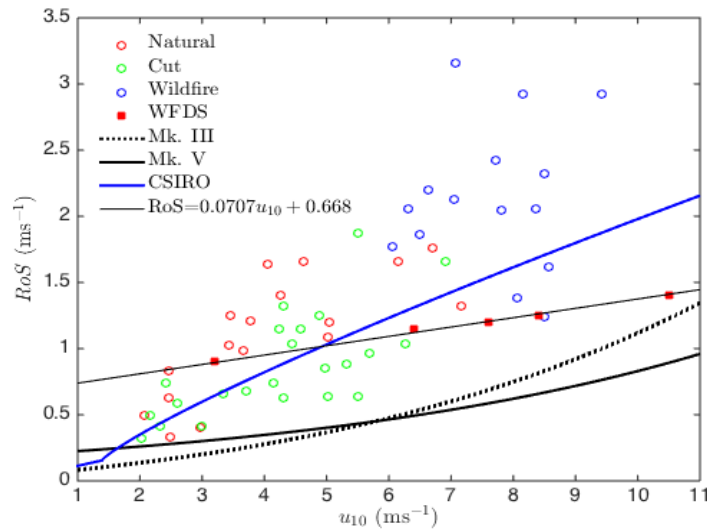
FIGURE 10: THE RATE-OF-SPREAD VERSUS 10 M OPEN WIND SPEED FOR THE SIMULATED GRASSLANDS, COMPARED WITH OPERATIONAL MODELS WHILST EXPERIMENTAL RESULTS OBTAINED BY CHENEY ET AL. [15] ARE PLACED IN THE BACKGROUND.
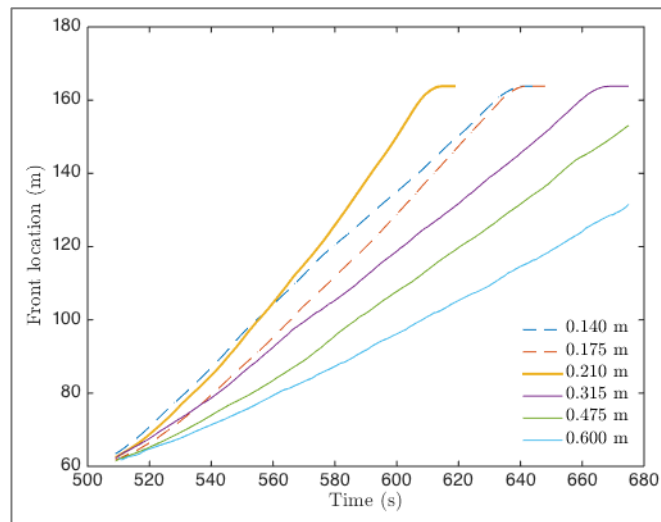

FIGURE 11: EFFECT OF GRASS HEIGHT IS SHOWN BY THE LOCATION OF FIRE FRONTS AS A FUNCTION OF TIME. 0.14 AND 0.175M CASES ARE IN BOUNDARY LAYER MODE OF PROPAGATION. 0.6, 0.475, 0.315 AND 0.21 M CASES IN PLUME MODE OF PROPAGATION. IN THE PLUME MODE, INCREASING GRASS HEIGHT IN THESE SIMULATIONS LEADS TO A DECREASE IN THE RATE OF SPREAD.

Simulation of heat fluxes on structures.

Australian building standard AS 3959 [3] provides mandatory requirements for the construction of buildings in bushfire prone areas in order to improve the resilience of the building to radiant heat, flame contact, burning embers, and a combination of these three bushfire attack forms. The construction requirements are standardised based on the bushfire attack level (BAL). BAL is based on empirical models which account for radiation heat load on structure.

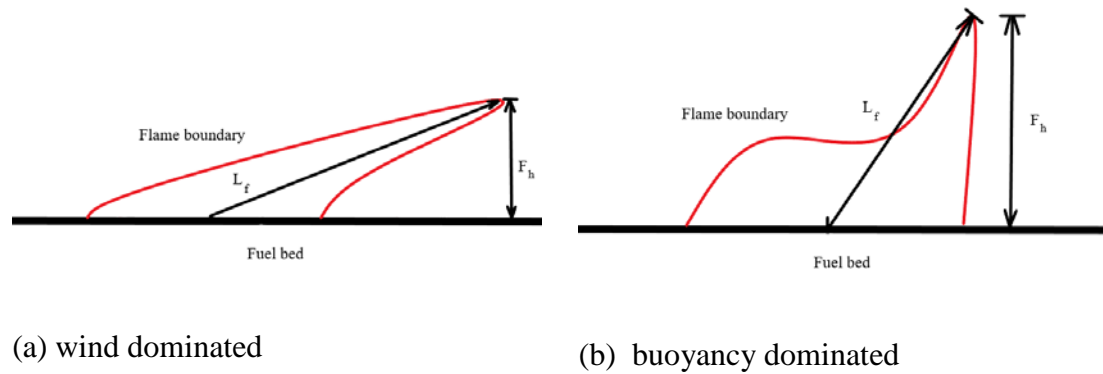(a) wind dominated   (b) buoyancy dominated

FIGURE 12 CARTOON SHOWING A SKETCH OF THE TWO DIFFERENT FLAME GEOMETRIES EXPECTED FROM THE TWO FIRE PROPAGATION MODES.

The prediction of the heat load on structure is a challenging task due to many influencing factors: weather conditions, moisture content, vegetation types and fuel loads. Moreover, the fire characteristics change dramatically with wind velocity leading to buoyancy or wind dominated fires that have different dominant heat transfer processes driving the propagation of the fire [14, 18, 19]. In the wind dominated mode, the shearing fluid flow (that is, the wind) dominates over the buoyant flow (the updraft from the fire plume). The flame is elongated and confined to a boundary layer structure as shown in Figure 12(a). In the buoyancy dominated mode, the updraft from the fire is sufficient to overcome the shearing forces of the driving wind and the flame becomes more vertical, see Figure 12(b). In the wind dominated mode, the flame height (F_h) is low and so the view factor will be small compared to the buoyancy dominated mode, however, because the fire plume is confined to a boundary layer, there will be a high convective heat flux downstream of the fire. In the buoyancy dominated mode the plume is vertical and therefore the convective heat flux ahead of the fire will be small compared to the wind dominated mode. On the other hand, because the flame is vertical, the radiant heat flux ahead of the fire will be high compared to the wind dominated mode.

The AS 3959 standard is developed with respect to a quasi-steady state model for bushfire propagation assuming a long straight line fire. The fundamental assumptions of the standard are not always valid in a bushfire propagation. The AS 3959 model predicts monotonic increase in flame height with increasing RoS and therefore, assuming flat ground, increased radiation load upon a structure. However, we hypothesise that if the fire becomes wind dominated the flame height will decrease and the corresponding increase in intensity may not be sufficient to ensure that the heat load on the structure increases with increasing wind speed.

We have conducted physics-based modelling to estimate the heat load on a model structure. In this work, we have conducted simulations to compare the radiation heat load upon a structure, as close as possible, from the fire scenario in AS 3959 predicted by the BAL set out in the standard, to the radiation heat load simulated by a physics based model. The idea is to assess the validity of the standard as it stands, rather than looking to extend the standard to include new features such as ember attack. Specifically, we have attempted to:

- Identify if the BAL classification values are supported by physics-based simulation,
- Assess the sensitivity of the radiation heat load to the wind speed, fuel load, and relative humidity and

- Examine the differences in heat load on a structure between buoyancy dominated fires and wind dominated fires.
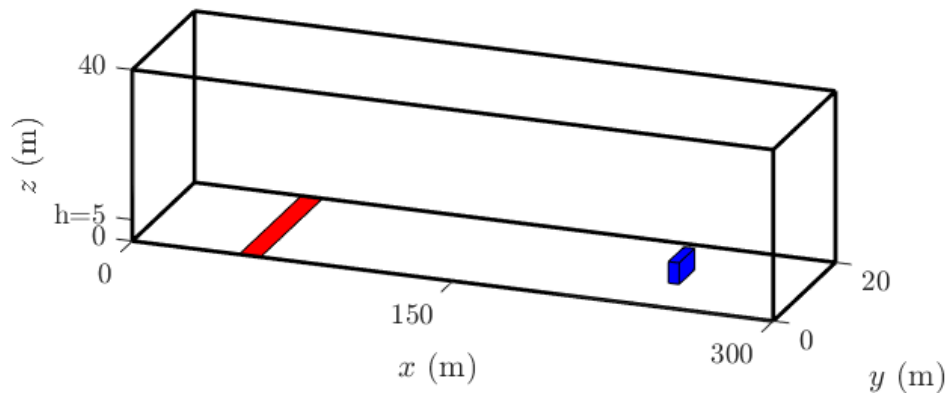

FIGURE 13:THE SIMULATION DOMAIN SHOWING THE LINE IGNITION SOURCE, AND THE HOUSE STRUCTURE

The simulations are as close to the AS 3959 standard as computationally practical. However, due to computational restrictions, the fire width is considerably reduced from 100 m to 20 m. However, if the radiative heat load predicted by a 20 m wide fire is larger than predicted by AS 3959, it is reasonable to assume that the 100 m wide fire will exceed the standard by a larger amount. For simplicity, we consider a grassland fuel at GFDI=50 to match the fuel class G in AS 3959. Further simulations are conducted to assess the effect of varying the driving wind speed, relative humidity and fuel load on the heat flux received by a structure and to determine if the different modes (wind dominated or buoyancy dominated) of fire propagation affect the radiative heat load upon a structure.

The simulation is conducted as shown in Figure 13. A structure of size 5m x 5m x 2.5m is located as shown in the figure. The structure is a solid object with no-slip boundary conditions and thermally inactive material properties. Therefore, no re-radiation from the structure to the fire is included in the simulations and combustion of the structure is not simulated; these assumptions are also implicitly made by AS 3959. The wind-only flow is firstly allowed to spin-up for a time of 300 s, to ensure a statistically stationary wind field throughout the domain. Then the fire was ignited at x=40 m from the inlet.

The quantities measured in the simulations are the radiative and convective heat fluxes located on the walls of the structure and the boundary temperature. The heat fluxes are measured at a single point on each face of the structure, although only the face of the structure nearest to the approaching fire front is relevant. Because the flame may be quite long and elongated, the surface fire front location may be significantly further away from the structure than the location of the flame tip (see Figure 12). We computed both surface fire front location and flame tip location with respect to the structure – to identify the sensitivity to two different measurements. The fire front location is a more robust measurement; the flame tip location is obviously sensitive to turbulent fluctuations and the flame tip location varies significantly over a short time scale.

First, we have conducted a basecase simulation which is as close as possible to an AS3959 scenario. Here U_{10} velocity is 45 km /hr (12.5 m/s), vegetation load is 0.375 kg/m^2 and relative humidity is 25%. The radiative and convective heat fluxes received on all surfaces of the structure as a function of fire front distance from the structure are shown in Figure 14.
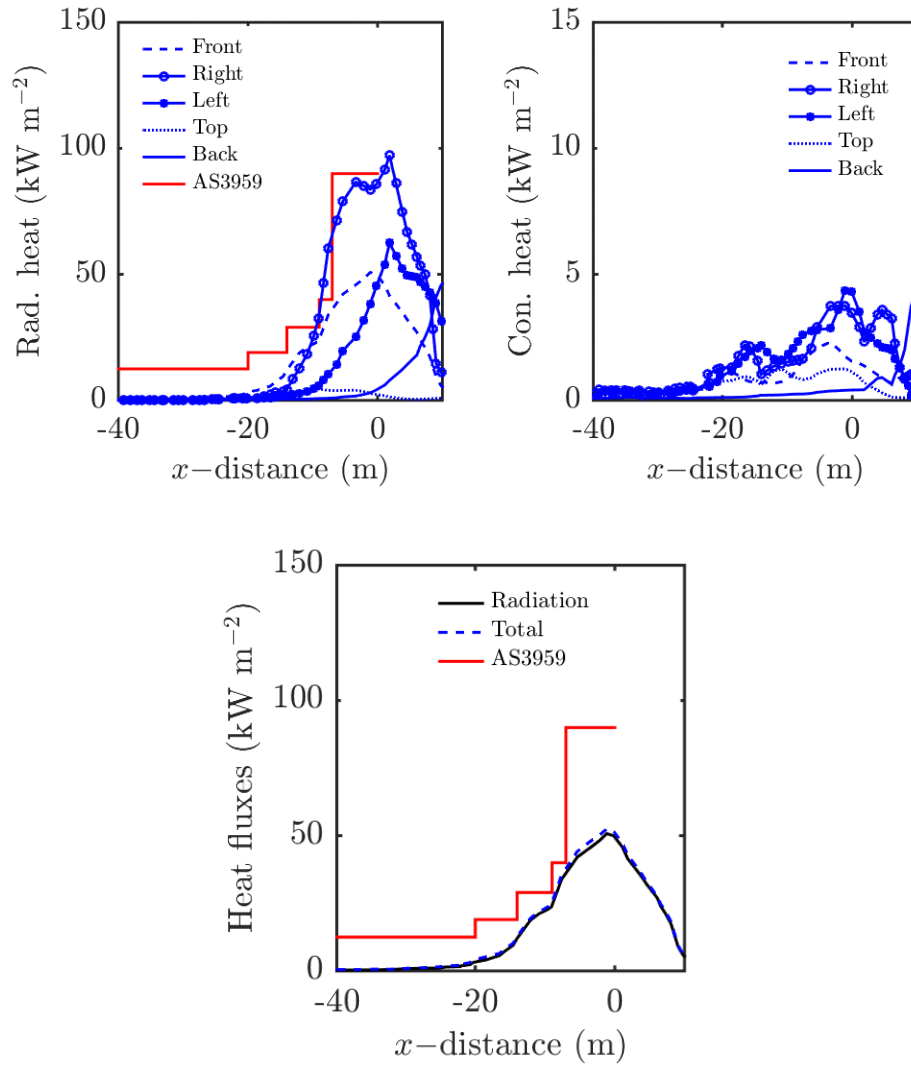
FIGURE 14: HEAT LOAD ON THE STRUCTURE (A) RADIATION (B) CONVECTIVE (C) COMBINED

The radiative heat flux on the structure is irregular, although some trends are observable. The heat flux on the front surface increases most quickly as the flame makes contact with the structure. The heat flux on the rear surface increases after the fire has passed the structure. The heat fluxes on the left and right sides both increase at the same distance (approximately -10 m) but the peak radiative heat load on the left hand side is much greater than on the right hand side. The asymmetry is likely due to a complicated wake behind the structure which leads to intensification of the fire on one side of the structure. While this phenomenon is interesting, a full investigation is beyond the scope of the present study. Furthermore, the peak of radiant heat flux, when the fire is in direct contact with the structure, is not important because the structure will likely ignite. The radiant heat flux on the top of the structure is minimal because the top surface is flat and not exposed to the flame.

The convective heat flux on the structure is approximately one order of magnitude less than the corresponding radiative heat flux on the structure and therefore negligible in terms of BAL in this case. However, this does not imply that the convective heat load on the structure is always negligible nor does this imply that the increased windload due to the convective plume can be neglected. The total heat flux, radiation plus convective, received by house structure at the front face is shown in Figure 15(c) and as expected, the contribution of convection to total heat load is negligible in this case.

The simulated heat flux follows the same trends as the BAL model,

- However, the BAL-12.5 and BAL-19 are apparently excessive. That is, the standard predicts heat flux far greater (between two and more than ten times) the simulated heat flux.
- However, the BAL-29 and BAL-40 regions agree with the simulation results.

Recall that the simulated fire is one fifth of the width of the fire modelled by AS 3959. The radiant heat load can be expected to increase with increasing fire width. Therefore, while the simulation results may apparently support the model in the standard, the simulated heat flux from a 100 m wide fire will likely exceed the standard. While this discrepancy may appear severe, the standard could be revised fairly easily.

(A) VARIATION WITH FUEL LOAD

(B) VARIATION WITH WIND SPEED
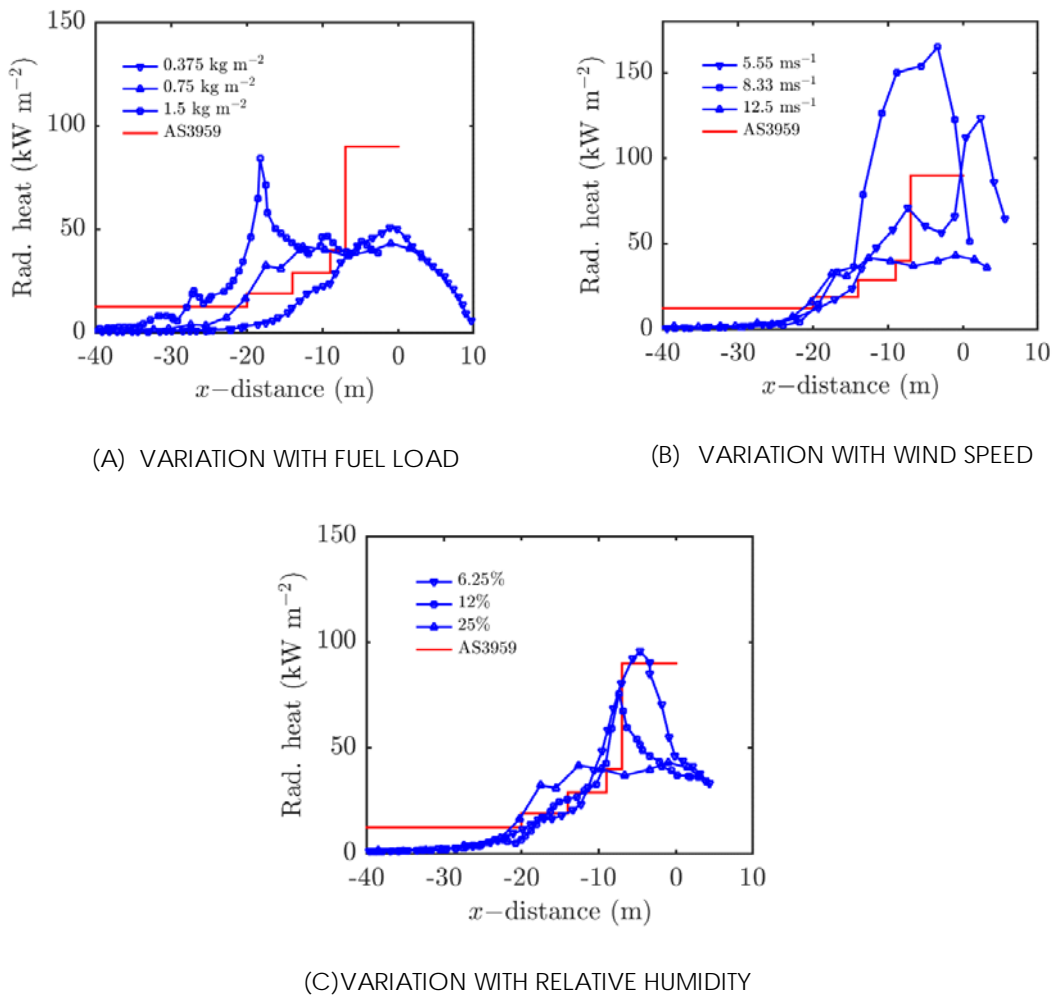
(C) VARIATION WITH RELATIVE HUMIDITY

FIGURE 15 COMPARISON OF RADIATION HEAT LOAD WITH AS 3959 DATA; (A) WHEN VEGETATION LOAD IS VARIED AND (B) WHEN WIND SPEED IS VARIED (C) WHEN REALTIVE HUMIDITY IS VARIED

To understand the sensitivity, we conducted two more simulations by varying vegetation load (0.75 and 1.5 kg/m^2) without varying wind velocity and relative humidity. All three cases were wind dominated. As expected increasing the fuel load increased the intensity of the fire, and subsequently the radiative heat flux at the structure should increase. The result is presented as Figure 15 (a). There is a peak in radiative heat flux in the highest fuel load case, at around x = -20 m. The exact cause of the peak is not investigated, but the peak in radiation heat flux corresponds to a peak in total heat release rate suggesting that fire has instantaneously flared up around that point.

To assess the sensitivity of driving velocity, three cases were simulated varying U_{10} as 20, 30 and 45 km/hr (5.55, 8.33 and 12.5 m/s), relative humidity was constant as 25% and vegetation load was constant as 0.75 kg/m^2. We found that 20 and 30 km/hr cases are buoyancy dominated, 45 km/hr case is wind dominated. As the wind speed increases slightly, the flame angle can become more acute to the ground, which increases the size of the pyrolysis region and hence increases fire intensity. However, if the angle becomes very acute, the flame can attach to the ground leading to a low flame height and a corresponding decrease in radiative heat flux at the structure. Figure 15 (b) shows the heat load with varying wind velocities; 20, 30 and 45 km/hr respectively. The figure supports the hypothesised effect of buoyancy dominated fire yielding higher heat loads at lower velocities.

To assess the sensitivity of relative humidity, three cases were simulated varying 25%, 12.5% and 6.25%, whilst U_{10} velocity was constant as 45 km /hr (12.5 m/s) and vegetation load was constant as 0.375 kg/m^2. The results (presented as Figure 15c) in these cases are complicated: the relative humidity (with constant fuel moisture content) does modify the radiative heat flux at the structure however the results are not completely systematic. The general trend is that lower relative humidity yields the peak higher radiative heat load. However, the 25% relative humidity case yields the highest radiative heat flux when $-20 < x < -10$ m. At $x = -15$m the 25% case gives radiative heat flux of approximately 30 kW/m^2, the 12% case gives radiative heat flux of approximately 22 kW/m^2, and the 6.25% case gives radiative heat flux of approximately 18 kW/m^2. At greater distances from the structure, $x < -20$ m, the order of the curves changes again. However, the difference in between the heat fluxes are relatively small for $x < -20$ m and this observation may simply be due to turbulent fluctuations in the fires or some other source of noise in the data. While relative humidity on its own does yield some changes in radiative heat flux at the structure, the changes are not entirely systematic. We therefore conclude that relative humidity largely acts as a proxy for fuel moisture content in the GFDI equation and further work is required to assess the effect of fuel moisture content upon the radiative heat flux at the structure.

Designing building standards is arguably a very difficult task. In the case of building in bushfire prone areas, the basic requirements of the standard are to ensure that a building is resilient to a realistic fire event and the standard is simple and straightforward to apply. Idealised simulations, such as those conducted here, can be used to revise existing standards simply by computing the radiant heat flux received at the structure under the situations outlined in the present standard.

Controlled physical experiments can also serve as a validation for proposed structural integrity discussed in AS 3959 in a bushfire attack. The controlled experiments have significant cost, risk and safety, which limits it utilisation. Numerical modelling reduces the cost, risk and safety in exploring the bushfire attack on structure. Previously, numerical simulations have been successfully applied to simulate experimental grassfires [14, 20]. Here, we have demonstrated that the same physics-based models can simulate the radiant heat load upon a structure. The computational cost required to simulate fire impact on a structure is currently too great to allow the possibility of simulating a proposed structure in a given location in detail. However in the future, simulation of fire impact on a proposed design may become part of the design and approval process.

For the data presented here, the idealised models included in AS 3959 were found to under predict the simulations results when the flame front is near the structure. Furthermore, the models in AS 3959 do not account for the differences between buoyancy

dominated and wind dominated fires. Given these limitations and the omission of any kind of ember attack model, in the AS 3959 the standard should be re-examined.

Because computational technology and physics-based simulation have advanced considerably since the standard was originally implemented, physics-based simulations of bushfire attack on a structure could be used to strengthen the standard. It is important to examine the limitations of the approach presented here. Firstly, it is unlikely that a house structure would be built in unmaintained grasslands; most houses have a garden with watered or mowed grass forming a buffer region from the fire. Nonetheless the simulations conducted here reflect the situations outlined in AS 3959. The present research only considers surface fuels whereas the standard is mostly concerned with elevated forest or shrub like fuels. In planning this study, it was thought that surface fuels were likely to be better predicted by the idealised model used by the standard. The geometry of the vegetation, the possibility of crown fuel involvement, and wind reduction due to the vegetation are expected to complicate the fire impact upon a structure. Similarly this study did not address the effect of sloping terrain on the fire spread and radiative heat load. Therefore a further study should be conducted in future to address these limitations.

Simulation of grassfires on various upslope

The principal objectives of studies in wildland fires are: to quantify fire danger and thereby developing fire danger rating systems and to develop models which enable the accurate prediction of fire spread. Currently the fire authorities and agencies use operational models based on empirical modelling to predict the rate of fire spread. However, these models have limitations in predicting fire behavior under a wide range of topographic and weather conditions and may not be able to account for all kinds of inhomogeneity, slope etc. Grasslands are often found on terrains with slope. This topographic feature can increase or decrease the rate of fire spread depending on whether the slope is upward or downward.
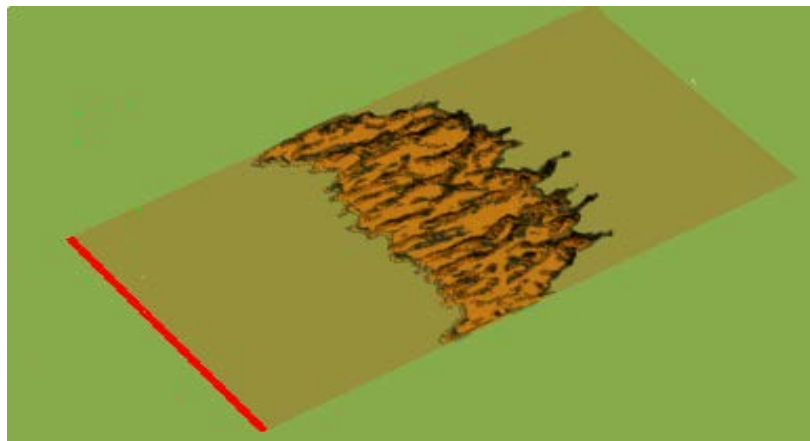

FIGURE 16: EXAMPLE OF FIRE SIMULATION

In this study, at first, a set of seven simulations have been conducted with constant wind speed (U_{10}= 12.5 ms^{-1}) and fuel conditions with varied slope angles. The simulations have been performed following the methodology of Moinuddin et al. [14], to analyze sensitivity of the results and to establish atmospheric boundary layer above the grassland within the simulation domain. The differences in this study are; this study uses a different domain size, straight line ignition protocol and turbulence is introduced at the domain inlet using synthetic eddy methodology (SEM) proposed by Jarrin et al [21]. Figure 16 shows an example of the simulated flame propagation, the dark green represents the

burnable material, the red line is the ignition line and the orange is the flame represented by isosurfaces of heat release rate per unit volume (HRRPUV).
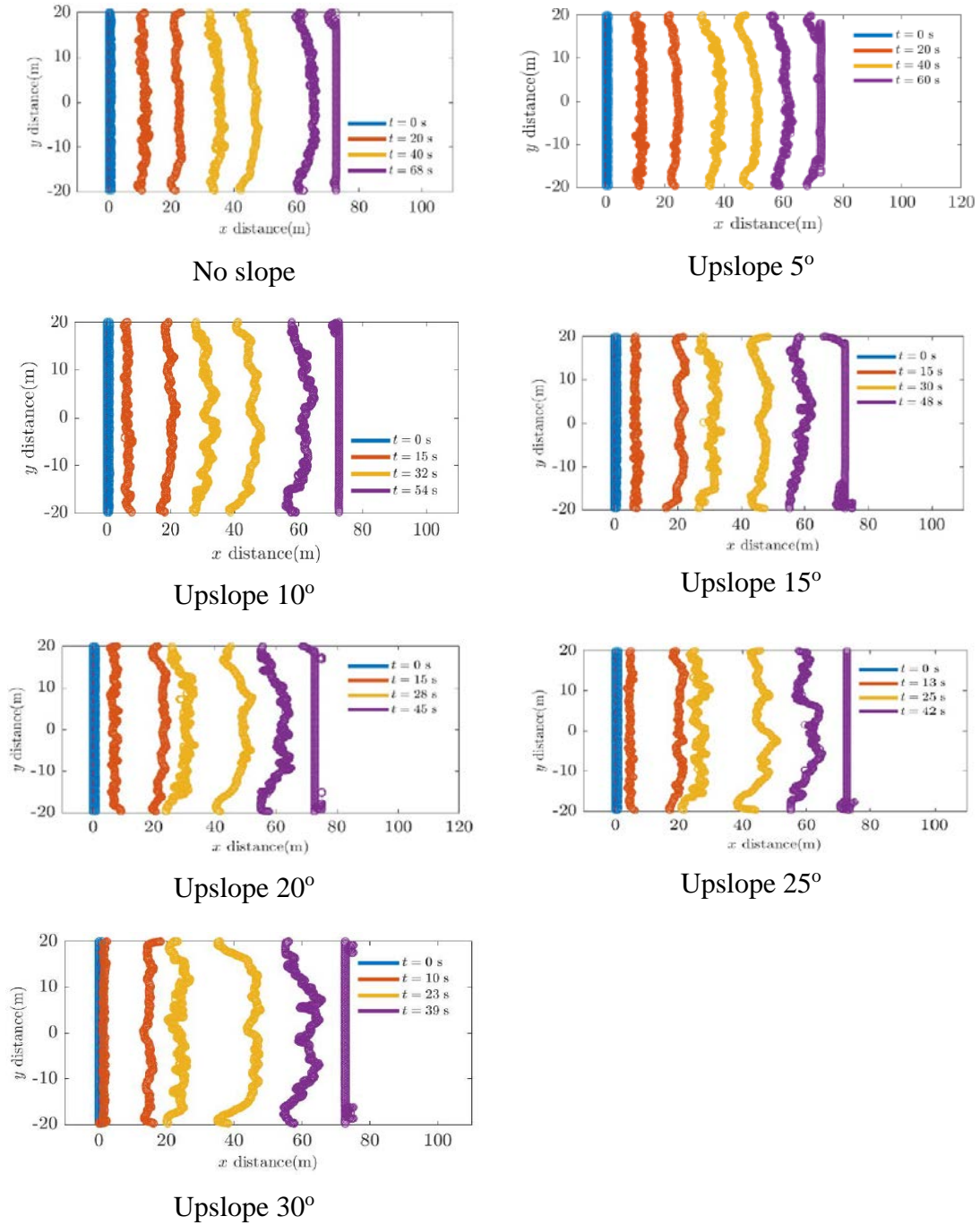

No slope

Upslope 5°

Upslope 10°

Upslope 15°

Upslope 20°

Upslope 25°

Upslope 30°

FIGURE 17: PROGRESSION OF ISOCHRONES

The simulation domain size is 360 m long x 120 m wide x60 m high. The burnable plot size is 80 m long x 40 m wide and 60m high, which is located at 160m from the inlet and there is a 120m long subdomain on the downstream of the plot before reaching an open outlet. Slope is implemented in the simulations by changing the magnitude of the components of gravitational force in the x and z directions so that $g_x = g \sin\theta$ and $g_z = g \cos\theta$, where g=9.8ms^{-2} and θ is the slope angle. Grid resolution 0.25x0.25x0.25m (longitudinal (x), lateral (y) and vertical (z) direction) is selected for the burnable plot following Moinuddin et al. [14] which achieved numerically converged solution for minimal variation of rate of spread (R). The line fire is of 40m width and 1m deep, aligned

23

with the leading edge of the burnable plot width. The fire is ignited simultaneously along the ignition line and lasted for 10 secs.

The isochrones (fire perimeters) progressions as functions of time from seven simulations are presented in Figure 17. Fire spread occurs from left to right. In these simulations, fire contour is defined as the region on the boundary where the temperature of vegetation is above the pyrolysis temperature 400K. Fire fronts are plotted at different times after the ignition when flame propagation moves towards the end of burnable plot. From the contour plots, it is observed that as the slope angle increases firefront becomes wider and reaches the end of burnable grass plot much earlier. Firefront reaches the end of burnable plot at around 68sec for no slope cases. For 5°, 10°, 15°, 20°, $25°$and 30° slopes, the firefront travel times are 60, 54, 48, 45, 42 and 39 sec, respectively. Firefront extinguishes once it reaches the end of the burnable material.

Firefront width for all cases are analyzed and plotted in Figure 18. Pyrolysis width as a function of time for all slope cases are presented in Figure 18(a). For each case, pyrolysis width increases as the firefront progresses from the ignition line, then it plateaus (i.e. reaches a quasi-steady state) and finally decreases. It can be observed that as the slope increases, the width of the plateau decreases and its magnitude increases. Quasi-steady head fire width verses slope angle is represented in Figure 18(b). These width values are extracted as the mean values after approximately 15 sec to 35 sec from ignition. These values are approximate for $25°$ and $30°$ slope cases as for these cases the firefront reaches the end of fire plot much quicker and reaches peak values much earlier than other cases. Hence for higher degree slope cases, a perfect steady pyrolysis width condition has not attained at any given time. It can be observed that the width of head fire increases linearly with the slope angle. Firefront width increases by approximately 25-30% for every 10° slope.
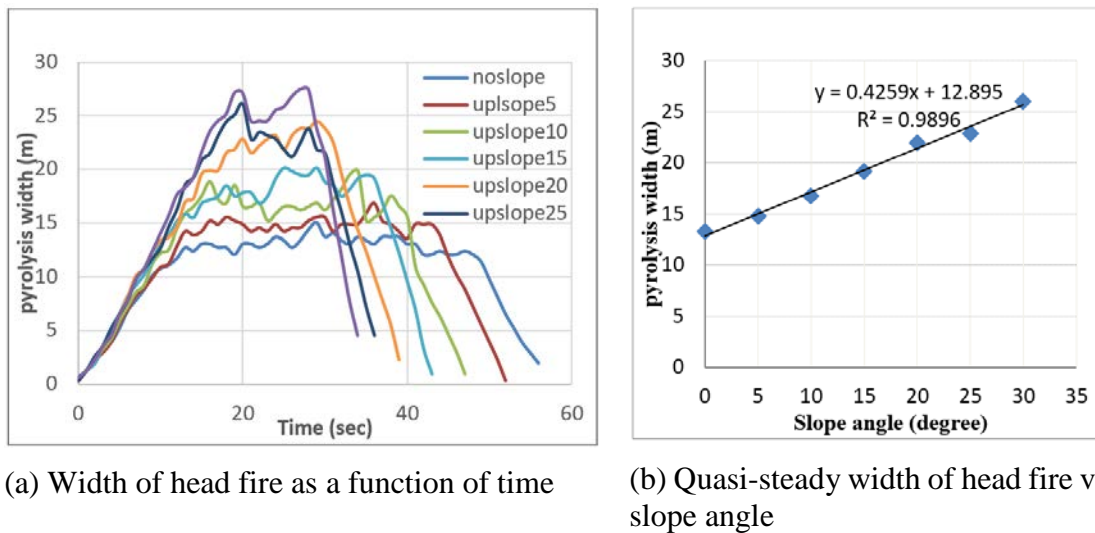

(a) Width of head fire as a function of time

(b) Quasi-steady width of head fire vs slope angle

FIGURE 18: PYROYSIS WIDTH

Firefront locations and Rate of Spread (R) calculations are presented in Figure 19. Firefront location is determined by examining the boundary centerline temperature as the fire moves through the grass regions. The locations of the firefront as a function of time are shown in Figure 19(a). Firefront is found to be moving faster with increase in slope angle. As the slope angle increases fire front location is farther. At a given time, the firefront location for the 30 degree slope case is farther by 35% than that with no slope

case. From the slope of the profiles of Figure 19(a) R is calculated and presented in Figure 19(b).

Rate of Spread derived from set of equations presented by Noble et al [4] for Mark 3 and Mark 5 version of the grassland fire danger meter are presented in Figure 4(b). Figure 19(b) shows the R values obtained from this study, plotted as an exponential curve, together with slope-corrected empirically derived R values with MK3 and MK5 models. At constant wind speed and fuel conditions, Equations are used to derive FDI for Mark 3 and Mark 5 versions and then the R value was calculated. R is then corrected for slope with slope correction factor as incorporated in Australian Standard AS 3959 [3] and given as Eq (6) to derive the forward Rate of Spread corrected for effective slope degrees.

$$R_{slope} = R \; x \; e^{(0.069 \; slope)} \quad \text{.... (6) when fires burning uphill (effective downslope)}$$
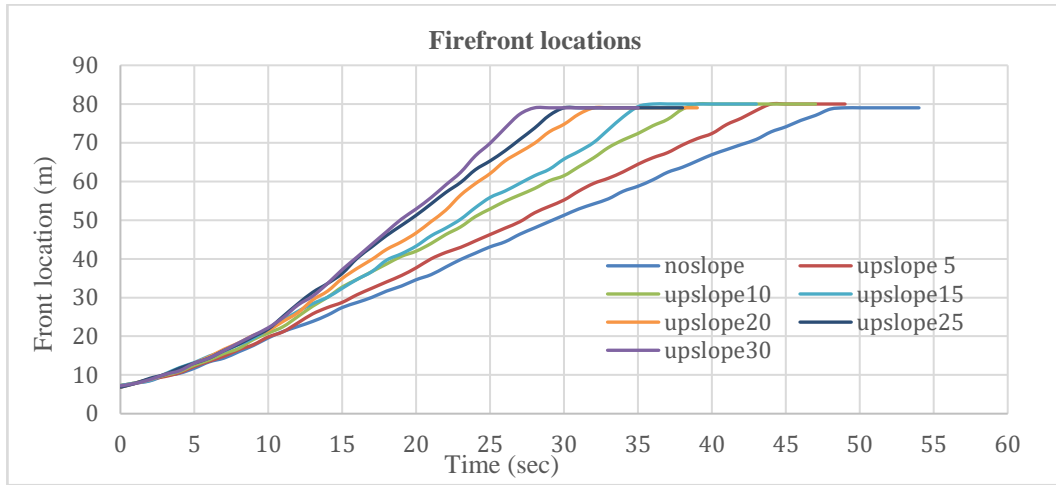
(a) Firefront location (m) verses time (s)
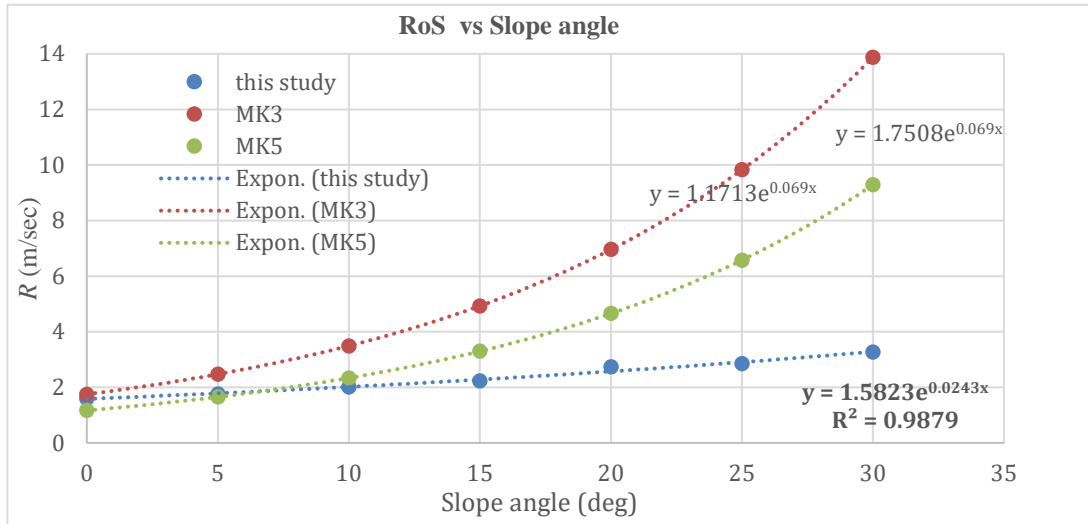
(b) Rate of Spread- slope angle correlation

FIGURE 19: FIREFRONT LOCATIONS AND RATE OF SPREAD CALCULATION

The rate of spread for zero slope case is comparable to the flat terrain simulations of Moinuddin et al. [14]. The minor differences are due to the use of SEM methodology and different ignition protocol. From Figure 20(b) it is observed that R values obtained from this study are found to be closer to empirically derived MK5 values for slope angle up to

10º. From 15º to 30º, *R* values from this study are observed to be higher with MK5 model. The difference widens as the slope angle increases. *R* values with MK3 are found to be significantly higher than those obtained from this study.

For some benign driving wind velocity, fires burning above 20º, the interaction of wind and topographic aspect can have significant implications on plume's behaviour and significantly affect heat transfer from the burning zone into unburnt fuel [18, 22]. Dold and Zinoviev [18] and Dupuy and Maréchal [23] conducted laboratory experimentation in separate studies and observed that flame or plume attachment leads to enhanced preheating of fuels upslope, ahead of the fire and resultant acceleration of the fire spread. If such phenomena occur, convective heat transfer significantly increases.

Plume behaviour for slope angles 10°, 20º and 30° (with U_{10}=12.5 ms^{-1}) are presented in Figure 20(a-c) which are obtained from WFDS' companion graphics software Smokeview. The dark green colour represents the burnable material, the red line is the ignition line and the plume indicated by the colour shading, which represents air temperature (red = hot, blue = cold). It is observed that at this wind velocity firefront travels very fast and in all cases plume is attached to the ground.

To observe the plume behaviour at lower driving wind velocity, we have conducted further simulations with lower U_{10} of 3 ms^{-1}. In Figure 20 (d-f), graphic representation of plume attachment at this wind velocity is presented. It is noted in Figure 20(d) that the fire's plume rises into air near the ignition line at 10º slope and at other slope angles, buoyant plume above the grass plot inclined at different slope angles. At higher slope, the plume is more inclined towards the ground. The interaction between the plume and terrain is captured clearly at 30° sloped terrain where the plume can be seen attached much ahead of the ignition line and the attachment is visible approximately up to the end of burnable plot. With higher wind velocity, the plume attachment behaviour happens at much lower slope angle as shown in Figure 20 (a-c). The overall results show similarity with the observations of [18, 22] that plume attachment occurs due to an interaction between the slope of the terrain and the fire's plume.

(a) 10° slope -wind velocity 12.5 ms^{-1}

(d) 10° slope -wind velocity 3 ms^{-1}

(b) 20° slope -wind velocity 12.5 ms^{-1}

(e) 20° slope -wind velocity 3 ms^{-1}

(c) 30° slope -wind velocity 12.5 ms^{-1}
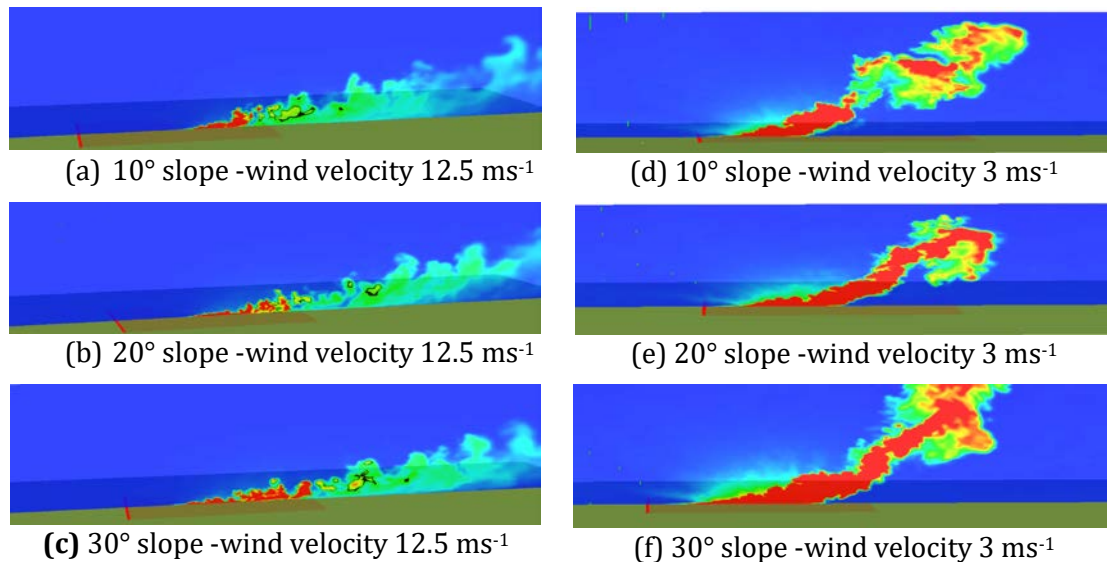
(f) 30° slope -wind velocity 3 ms^{-1}

FIGURE 20: PLUMES EMANATING FROM GRASS PLOT AT 10°, 20°AND 30° SLOPE -WIND VELOCITY 12.5 M/SEC

The study conducted so far includes simulations with upslope scenario. Further simulations are to be conducted with different U_{10} velocities as well as downslope scenario to understand the effect of wind and slope on fire spread rate.

Simulation of grassfires with PenaBlending Method

The wind is the most influential environmental variable that effects the wildland fire behaviour as explained by [17, 24]. A faithful representation of atmospheric boundary layer is required in order to confidently reproduce the rate-of-spread and intensity of the fire, the heat transfer to unburnt vegetation, and the transport of smoke and combustion product away from the fire ground. The inlet and initial conditions prescribed for the simulation preferably lead to a realistic flow over the fire ground which does not nonphysically develop in space or time. There are various methods available to generate wind field in the physics-based model Fire Dynamics Simulator (FDS) which we termed as the traditional methods of wind field generation. The conventional methods of wind field generation are either the 'Wall-of-wind' method where an unperturbed inlet profile with a roughness-trip is used (wind1) or the by embedding artificial turbulence at the inlet known as Synthetic Eddy Method (SEM) [21] (wind2). Each of these methods require substantial computational time for the statistically stable wind to develop over the simulation domain. The third method is a mean-forcing method for neutral atmospheric conditions (wind3).

The initial mean flows for the fire simulations can be generated with relative ease. For example, we can use the log-law model (analytical approach), a mass-conserving perturbation model or a large scale numerical weather prediction model as initial mean flow condition. Each of these methods has an associated computational cost, with the analytic mean model being the cheapest, the perturbation method has intermediate cost, and a large scale simulation is extremely costly. However, as discussed before, this cost needs to be kept minimised like using the less costly methods (analytical methods or reduced models) or re-using a precursor simulation multiple times). The challenge is to implement these boundary conditions in a physics-based fire model. Pena-Blending Method (wind4) helps in implementing such boundary conditions in FDS, following [25]. This method inserts an artificial forcing term in the Navier Stokes equation to force the velocities to the desired values.

Unlike the traditional wind generating models, the PenaBlending method sets both inlet and outlet conditions, hence it is designated as initial conditions. It sets the initial conditions of the fire simulations to the initial conditions prescribed by the external model or simulation. This can be achieved by implementing a one-way coupling algorithm in FDS. The external data obtained can be referred to as pSim data, which can be a specified analytic profile (eg, generated from Matlab) or come from some other reduced models of wind fields, or some experimental wind data. This data can be conducted over a largers domain with coarser resolution in time and space than the simulation domain, if required and hence incur minimum computational cost (some few seconds). The pSim is enforced as an initial condition first which is known as penalisation region and then a specific transition region, known as the blending region is applied to smoothly transition the simulated flow in the fire domain to the flow enforced on the boundary. This is based on the blending method as proposed by [26]. Currently, we have implemented the Pena-Blending Method along x-direction only.

The pSim may have a coarser grid than the FS domain. In such a case, these are required to be interpolated in order to achieve the same grid resolution as the simulation domain. The finer scale eddies generated within the fire simulation domain may not match with eddies that are applied as a forcing in the penalisation region. This may give rise to inconsistency in the turbulent structures at the inlet and outlet coupling regions. Blending region allows a smooth transition of eddies at vicinity of the coupled boundaries. At the inlet of the simulation domain, eddies from the pSim are enforced by

coupling. They travel into the simulation domain by advection and give rise to new turbulent structures as the simulation progresses. These new structures are transported to the nested outlet. If there is no blending region used, then there are inconsistent eddies at the coupled boundaries. For current study, a preprocessing step is conducted to process the pSim data into a number of files for each mesh, each file containing the velocity data for the penalisation and blending regions on the same grid as the simulation domain. In case of a timestepping simulation, the intermediate data at arbitrary times between the subsequent timesteps of pSim are obtained. These data may have a coarser grid than that required for the FDS domain. These data are then converted to the required grid resolution using linear interpolation method, so that it can be fed to FDS at required time-steps. The penalisation and blending regions are imposed using a straightforward forcing term in the Navier-Stokes equation.
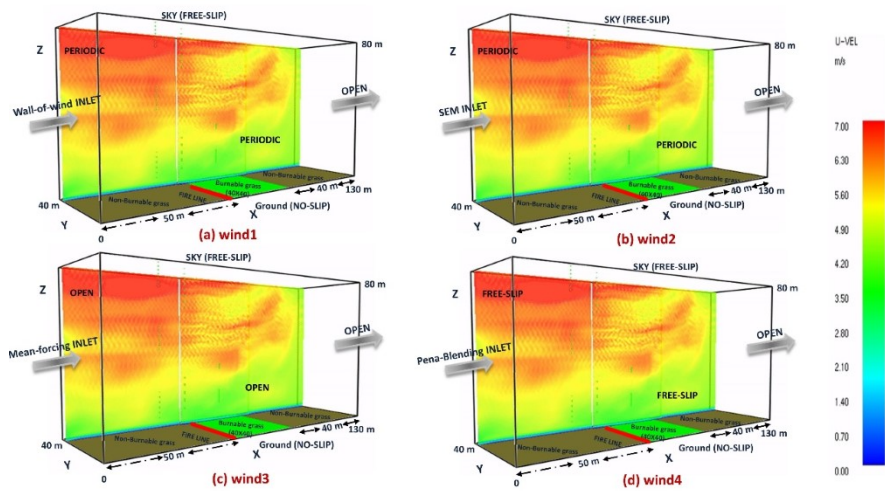

FIGURE 21: A GENERALISED SCHEMATIC REPRESENTATION OF THE DOMAIN SET-UP WITH BOUNDARY CONDITIONS OF WIND CASES FOR (A) WIND1; (B) WIND2; (C) WIND3; (D) WIND 4, INCLUDING THE EXTERNAL DIMENSIONS, FIRE-LINE, FIRE PLOT AND A SLICE OF ESTABLISHING ABL. THE FIRE SIMULATIONS HAVE A SIMILAR SET-UP.

The domain used has a dimension of 130 m X 40 m X 80 m. The domain is divided into a range of sizes. To avoid any instabilities or error in simulation, the aspect ratio is maintained less than 2m for each grid cells. For wind simulations, an uniform grid-resolution of 1 m is set for all the three directions (x,y,z) . For the fire simulations, an uniform grid-resolution of 0.25 m is maintained on the fire-plot upto z = 6 m. The rest of the domain has an uniform grid-resolution of 1m. The burnable grass plot of dimension (40 m X 40 m) is located at x=40 m from the inlet, followed by a non-burnable grass plot of 50 m downstream before reaching the outlet. Enough distance is maintained in the up-stream of the fire plot to let the wind develop and reach a required state for starting the fire simulation. Similarly, enough distance in down-stream is also maintained so that the plumes can travel and escape the domain and finally extinguishing the fire completely. An infinitely long line fire is simulated following [27] in the cross-stream direction. This means that the line -fire is extended throughout the width of the domain. This results in fire properties like depth of fire front, flame length, flame angle and rate-of-spread (RoS) of fire not varying along the cross-stream direction (in this case the y-direction).

The simulations carried out are done in neutral atmospheric stability conditions, which means there is no effect of applied surface heat flux on any of the simulations. The PenaBlending Method sets the boundary conditions of the simulation domain similar to

the boundary conditions of the external model or simulation (pSim) as discussed previously. Currently, the PenaBlending Method is applied only along the x-direction. Hence, the boundary conditions along x-direction are set as per pSim. In case of both wind and fire simulations, a free-slip or no normal velocity conditions are used in cross-stream directions, and at the top of the domain. The ground is prescribed as a solid boundary and is set to no-slip. The ground has vegetation comprising burnable and non-burnable grass. The simulations using wall-of-wind method (wind1 and fire1) have an inlet of a 1/7- power law wind profile and an open outlet. The lateral or cross-stream boundaries are set to be periodic along with a no-slip and free-slip boundary conditions at z = 0 and z = 80 (for small domain) and z = 100 (for large domain) respectively. Both the SEM (wind2 and fire2) and the mean-forcing (wind3 and fire3) methods have a log-law mean flow inlet profile. The domain set-up can bedepicted in Figure 21.

(a) The mean-velocity profiles

(b) Semi-log scale mean velocity profiles

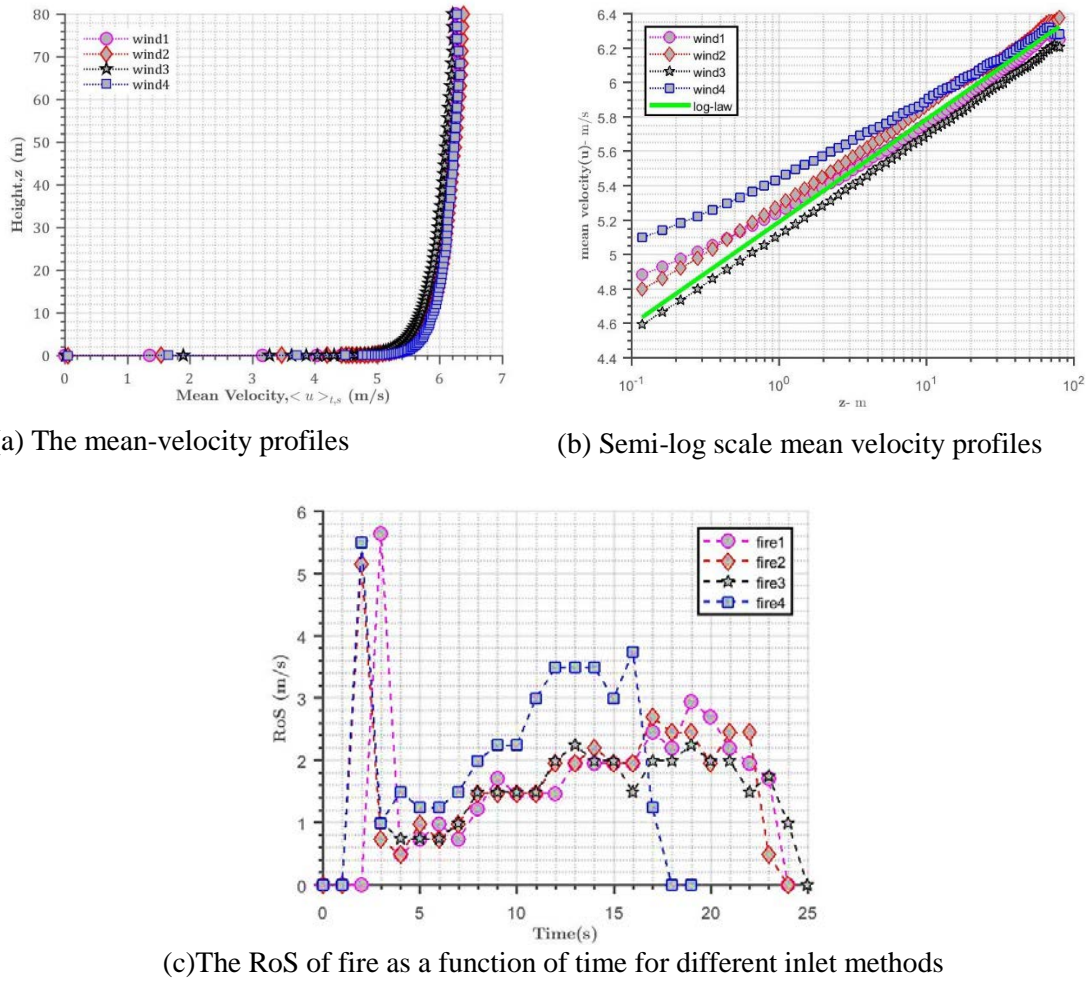(c)The RoS of fire as a function of time for different inlet methods

FIGURE 22: COMPARISON OF VARIOUS FIRE AND WIND PARAMETERS OF PENABLENDING METHOD WITH THAT OF THE TRADITIONAL METHODS

In order to verify the nature of the wind profile obtained using PenaBlending method, we have plotted the mean velocity profiles for all the four wind cases, as shown in Figure 22(a). Here the change in the u-velocity is plotted against the domain height averaged in space and time. An average u-velocity at height 10 m, referred to as U_{10} has been maintained at ~ 5.5 m/s for all the cases. These profiles are obtained at 50 m upstream of the inlet and averaged over the fire plot of 40 m X 40 m. It is observed that the velocity profile of the wind simulation using PenaBlending Method(wind4) reasonably collapse on those obtained from the reference cases, using the traditional method (wind1, wind2, wind3) with an expected wind profile for both the domains [14]), hence verifying a

correct implementation of the wind development using the PenaBlending Method. To verify the robustness of the ABL simulation, semi-logarithmic plot of mean-velocity profiles have been shown in Figure 22(b). These profiles are taken over the fire-plot, similar to the mean velocity profiles. It is observed that all the four profiles reasonably collapse on each-other from z = 10 m onwards with some variations and a logarithmic layer is observed. The log-law plotted is observed to be parallel and fitting to the mean-velocity profiles. In the current study only the U_{10} at the inlet has been tried to match to see the developed wind-field for comparison. It is observed from these profiles that the u2 velocity for different cases varies prominently. The same wind field is used to carry out the fire simulation cases.

To campare the fire simulation using PenaBlending Method, the RoS (rate-of-spread) has been compared. Figure 22(c) shows the RoS comparisons for all the fire cases. It is observed that all the three fire cases (fire1, fire2, fire3) reaches the end of fire-plot by ~24 seconds. Near the start of fire, the RoS is maximum for all these case and then reaches a quasi-steady state of ~2 - 2.5 ms^{-1} before the fire reaches the end of fire plot. In case of fire4, the RoS increases up initially and then reaches a quasi-steady state of ~ 3- 3.5 ms^{-1} and then reaches the fire-plot end within~18 seconds. Moinuddin et al [14] discusses the fact that a minor differnce in wind speed and direction can have a considerable effect in the simulation results. Figure 22 (b) shows that there are some differences in the mean velocity fields for all the cases. Therefore it can be concluded that the differences introduced in the wind fields by the different inlet conditions leads to the variation in the RoS for the fire simulation cases.

MODELLING OF FIREBRAND TRANSPORT

This work seeks to study the transport of ember particles across realistic forest edges. We seek to compute and characterise the final ember landing distributions, with an eye to developing operational models of ember attack. Such a model will inform scientifically sound forecasts of ember risk from bushfires. Improved forecasts will mitigate the potential risks posed by embers to human lives and properties on the WUI.

(a) highlighting the canopy and ember plane location

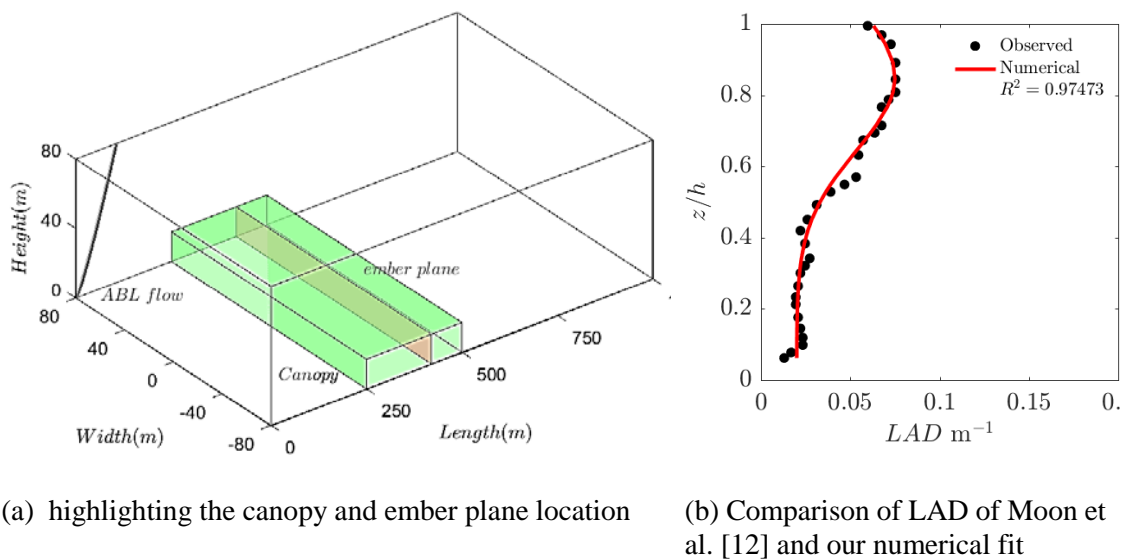(b) Comparison of LAD of Moon et al. [12] and our numerical fit

FIGURE 23: COMPUTATIONAL DOMAIN WITH CANOPY AND EMBER PLANE LOCATION AND LAD PROFILE

We simulate the transport of Lagrangian particles away from a modelled fire within a forest canopy. The particles are tracked across the forest edge and the distributions of embers on the ground were characterised by mean and variances in the x and y directions. Different ember shapes are simulated to understand how ember shape effects the spotting distance and lateral dispersion of embers.

The computational domain used in this study is shown in Figure 23(a). The simulation domain is 1000m long, 160m wide, and 80m high. The forest canopy is starts at x= 250 which is 250m long, 160m wide and 17m high. It is modelled as a region of aerodynamic drag, where the drag force varies with the leaf area density (LAD) profile [19]. LAD is generally heterogeneous in the vertical direction and varies with the type of vegetation. However, for simplicity, we assumed LAD to be constant in time and we also assumed that LAD does not change along the length and breadth of the forest.

We used the LAD profile of the open woodland forest category measured by Moon *et al.* [18]. We fit a Gaussian function (Eq 7) to the observed LAD data as presented in Figure 23(b). The LAD profile fitted to the data is

$$LAD_{num} = 0.055e^{-(\frac{(z^*-0.85)^2}{0.085})} + 0.02 \, , \quad z^* = \frac{z}{H} \, . \tag{7}$$

An ember generation plane is defined at 170m inside the canopy which is highlighted with red in Figure 23. A stationary fire is modelled at the base of the ember generation plane by a region of specified fire intensity at 4714.6 kW/m. The intensity of fire is determined from the data provided for dry sclerophyll eucalyptus by Cruz *et al.* [28]. Two shapes of ember particles of density 225kg/m^3 are ejected from the ember plane, (a) square disc and (b) cylindrical shaped embers.

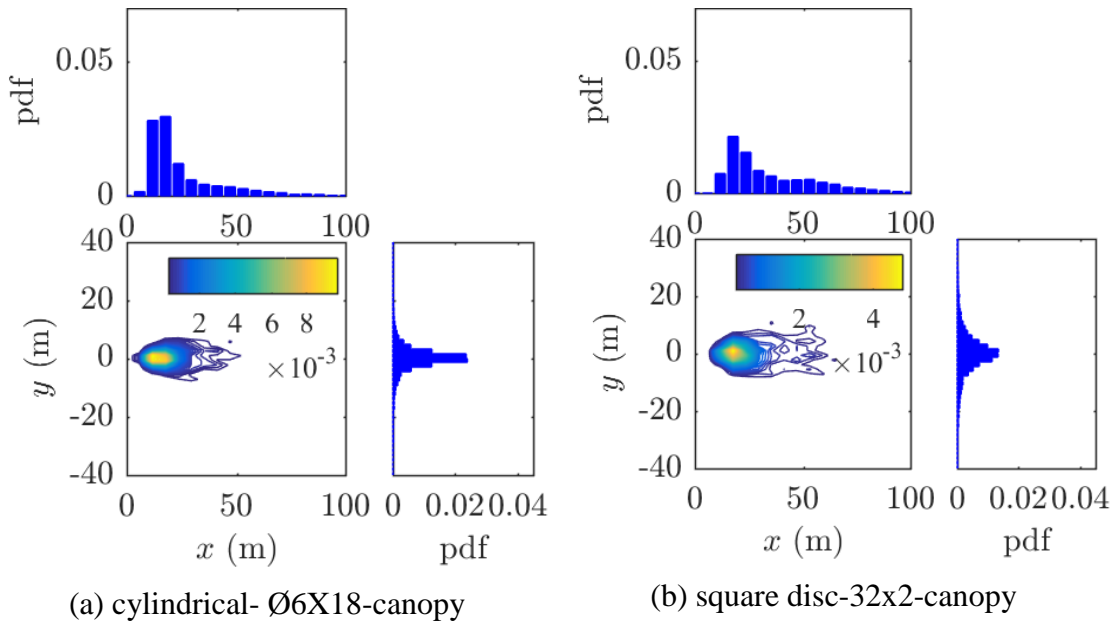(a) cylindrical- Ø6X18-canopy   (b) square disc-32x2-canopy

FIG. 24: SPATIAL DISTRIBUTION FOR CYLINDRICAL PARTICLE AND SQUARE DISC EMBER PARTICLES AT INITIAL TEMPERATURE OF 411°C

Three initial particle dimensions for each shape is considered based on the observed ember sizes [29-31]. The sizes considered for two shapes are: square-disc (Ds1-3) (length and thickness) (10X2.5, 32X2, and 32X4mm) and cylindrical (Cyl1-3) (diameter(Ø) and

length) (Ø6X12, Ø6X18, and Ø3X18mm). This yields sphericities of 0.64, 0.338, 0.64, 0.665, 0.832, and 0.779, for Ds1-3 and Cyl1-3 respectively.

The wood material typically ignites around 360-420°C [32] so initial ember particle temperatures is assumed to be 411°C. The density of the particles is constant throughout the simulations. The ember particles are divided based on its initial height, two regions on the ember plane representing bark (h=0 to 10m) and crown (h=10 to 17m). The simulated wind field is allowed to develop to a statistically steady state for a simulated time of one hour, before particles are injected. After the background flow is steady, four thousand ember particles of each shape and size are injected on the ember plane.

The ember distributions for the embers originating in the crown section of the forest canopy are presented in Fig.24. for two example cases: cylindrical Ø6X18 and square-disc-32X2. The lateral dispersion of ember particles is computed as the signed difference between the final and initial y-locations of the particle, so the mean distance in the y-direction (lateral dispersion) is zero. The bivariate probability distribution function (pdf) of cylindrical embers is estimated from the histogram of final ember location normalised so that the volume under the surface is one. The pdf of embers shows only the first impact location on the ground; bouncing of ember particles is not considered.
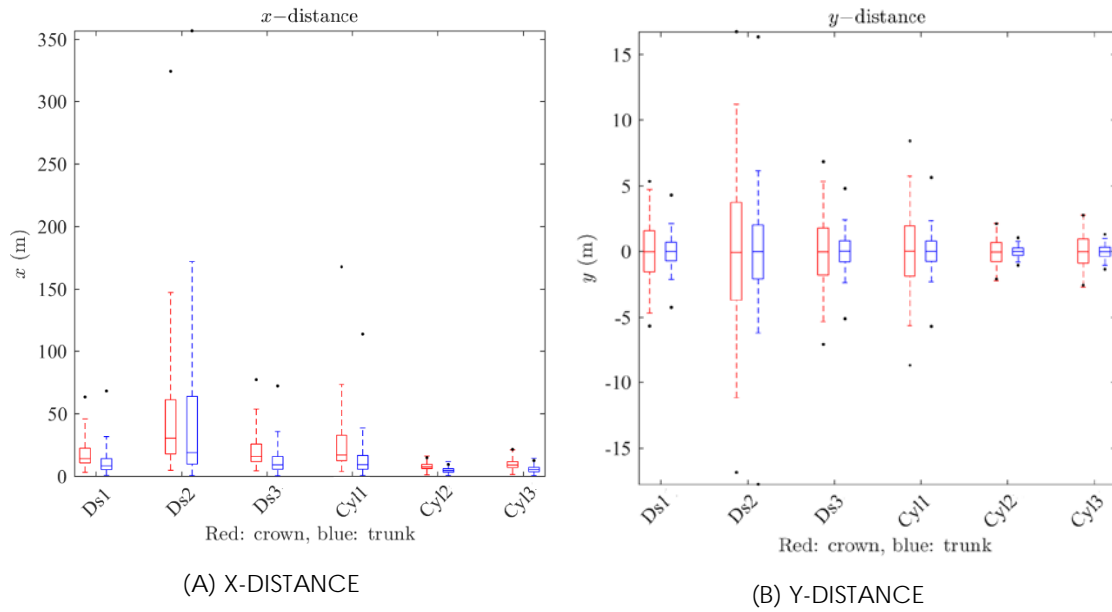

(A) X-DISTANCE

(B) Y-DISTANCE

FIG. 25: VARIATION OF MEDIAN, FIRST AND THIRD QUARTILES IN STREAMWISE (X-DIRECTION) AND CROSSWISE DIRECTION (Y-DIRECTION). BLACK DOTS DENOTE THE MAXIMUM DISTANCE UP TO WHICH 95% EMBER FALLS

The marginal pdfs in the x- and y-directions are computed by summing the bivariate pdf in the y- and x-directions respectively. The contours of the bivariate pdf, the x- and y-marginal distributions of cylindrical embers are shown in Fig. 24a. The same distributions for the square disc particles-32x2mm are shown in Fig. 24b. The observations show that cylindrical ember particles are more concentrated compared to square disc ember particles, which can be seen from the colour scale used in Fig 24. The distributions of embers in x-direction are observed to be qualitatively similar with the field study in Project Vesta for short-range embers [33]. Fig. 25 (a) and (b) are box-and-whisker plots of the x- and y-distances that the particle travels. The box-and-whisker plots shows the variation in the distributions of all six type of embers generated from crown and trunk section on the firebrand plane. The maximum spotting distance of ember in our study is

defined as the maximum distance up to which 95% of the ember falls which are shown by black dots in Fig 25.

Square disc embers found to generally travel farther compared with cylindrical embers and the square disc ember particles are observed to disperse more compared to cylindrical embers in crosswise (y-) direction. The dispersal of the embers will depend on both the mass (given by the volume of the particle, because the density of the particle is constant) and the sphericity of the particle. The square disc particles have significantly smaller sphericity compared to the cylindrical particles and consequently the square disc particles are more dispersed than the cylindrical particles. The initial height of the ember appears significant to the final ember distribution. In almost all cases, the embers released from the trunk area travel a shorter distance than the embers released from the crown.

We have demonstrated that physics-based simulations can be used to study short-range embers transported away from a fire. The x-distance results are qualitatively similar to the observations made in Project Vesta [33]. The shape of the ember particle critically affects the maximum spotting distance and the dispersion of the particles. Future work will investigate the effect of the canopy type on ember transport and lead to operational models for short-range ember transport.

PUBLICATIONS

Journal Papers

In this year, we got three journal papers published/accepted for publication:

1. Simulation study of grass fire using a physics-based model: striving towards numerical rigour and the effect grass height on the rate-of-spread" (by Moinuddin, Sutherland and Mell) is published in *International Journal of Wildland Fire*.

Simulation study of grass fire using a physics-based model: striving towards numerical rigour and the effect of grass height on the rate of spread

K. A. M. Moinuddin [A] [B] [E], D. Sutherland [A] [B] and W. Mell [D]

+ Author Affiliations

International Journal of Wildland Fire 27(12) 800-814 https://doi.org/10.1071/WF17126
Submitted: 21 August 2017 Accepted: 25 September 2018 Published: 2 November 2018

2. Physics-based simulation of heat load on structures for improving construction standards for bushfire prone areas (by Khan, Sutherland, Wadhwani and Moinuddin) [34] is accepted for publication for a special wildfire edition of *Frontiers in Mechanical Engineering*.

ORIGINAL RESEARCH ARTICLE Provisionally accepted The full-text will be published soon. Notify me
Front. Mech. Eng. | doi: 10.3389/fmech.2019.00035

Physics-based simulation of heat load on structures for improving construction standards for bushfire prone areas

Nazmul Khan [1, 2], Duncan Sutherland [1, 2, 3], Rahul Wadhwani [1, 2] and Khalid Moinuddin [1, 2*]

[1] Victoria University, Australia, Australia
[2] Bushfire and Natural Hazards Cooperative Research Centre, Central Queensland University, Australia
[3] University of New South Wales Canberra, Australia

3. Modelling of tree fires and fires transitioning from the forest floor to the canopy with a physics-based model (by Moinuddin and Sutherland) [35] is accepted for publication in *Mathematics and Computers in Simulation.*

Conference Papers

In this year, we got six conference papers published/presented:

1.   The first paper, entitled "Large eddy simulation of flow over streamwise heterogeneous canopies: quadrant analysis" by Sutherland, Philip, Ooi and Moinuddin [36]. In this study, large eddy simulation (LES) results of flow simulation over heterogeneous forest canopies are presented. Each simulated forest consists of equal-sized strip canopies which alternate in the streamwise direction between sparse and dense leaf area density

2.   The second paper is entitled "A comparative study of wind fields generated by different inlet parameters and their effects on fire spread in Fire Dynamics Simulator" by Roy, Sutherland, Khan and Moinuddin [37].

3. The third paper is titled "Direct Numerical Simulation of confined wall plumes" by George, Phillip and Ooi. This fundamental study mimics the situation where there is a fire very close to a wall in a room and we investigate how dynamics and the physics of how quickly the smoke from the fire plume fills up the room.

21st Australasian Fluid Mechanics Conference
Adelaide, Australia
10-13 December 2018

Direct Numerical Simulation of Confined Wall Plumes

Nitheesh George, Jimmy Philip and Andrew Ooi

4. Dr Duncan Sutherland presented a paper titled "Simulations of the effect of canopy density profile on sub-canopy wind speed profiles" at AFAC 2018 conference [38]. Wind speed profiles through canopies with various shaped (vertically variant) LAD were presented.

5. Associate Professor Khalid Moinuddin presented a paper titled "Simulated transport of short-range embers in an idealised bushfire" [39] at 6th International Fire Behavior & Fuels Conference. The presentation covered the results and discussion presented in pages 29-31 of this report.

6. Dr Duncan Sutherland presented the paper "Simulations of surface fire propagating under a canopy: flame angle and intermittency', (by Sutherland, Philip, Ooi, and Moinuddin) at the International Conference on Forest Fire Research in Portugal in November 2018. The results of simulations of a wind-driven surface fire entering, propagating through, and leaving a region of aerodynamic drag was presented. The study is motivated by the need to understand how fires entering forested regions adjust to the lower wind speed inside the forest. We will discuss the transitions in flame angle that occur as the fire propagates under the forest. For lower driving wind speeds the rate-of-spread of the fire is largely unaffected by the canopy, however, for the higher driving wind speeds the fire appears to transition from a wind-driven mode, characterised by a low flame angle to a buoyancy-driven mode, characterised by a nearly vertical flame.

THE PROJECT - EVENTS

EFFECTIVE ENGAGEMENT

End user discussion

Given that the Lead End User agency is the RFS NSW and we are a Melbourne-based research group, mos of the end-user engagement took place during various national conferences and via email/ telephone.

During AFAC 2018 conference in Perth in Sep 2018, Dr Nazmul Khan gave two presentations to members of RFS NSW (End-users):

- Roadmap for Assessment of AS3959 [3] by physics based modelling
- Grass fire modelling

While both presentations involve grassfire modelling, the former emphasises on inclusion of firebrand risk. We highlighted our developed expertise in grassfire modelling as well as modelling of transport of firebrands. Our goals are:

- Assessment of heat and firebrand loading on structures
- Investigation of different mode of heat transfer
- Long term goal of firebrand transport simulation at field scale and generate correlations
    - in terms of particle number, size, shape and mass as function of fire intensities
    - need to relate firebrand landing distribution to the local fire behaviour
- The correlations (parameterization) to be used in Phoenix, FARSITE, Prometheus etc.
- Investigate strategies to include firebrand flux in AS3959
    - By mapping firebrand and heat flux on structures
    - By investigating propensity of house loss due to firebrand and heat flux on structures
- Potential Risk Modelling –Estimation of fire breaks etc.

We received some very useful feedback from Dr Stuart Matthews of RFS, NSW.

During AFAC 2018, A/Prof Khalid Moinuddin discussed with Dr Adam Leavesley at ACT Parks and Conservation Service about possible collaboration on utilization of our sub-canopy wind research. The utilization goal of this research is to generate wind reduction factor (WRF) to calculate Forest Fire Danger Index, FFDI (and rate of spread). Eventually, we would like to have a map of WRF – like the map of LAI which can be found from [13]. Fire behaviour analysts will be able to use this information. This may be embedded in Pheniox or SPARK toolkit. Dr Leavesley referred us to Prof Albert Van Dijk and Dr Marta Yebra at Australian National University (ANU) who are developing fuel structure and flammability map using satellite imagery. ANU group is willing to collaborate and Dr Sutherland being in Canberra already met Dr Yebra and collected some data. Dr Sutherland also met Mr Rick McRae at ACT Parks and Conservation Service to discuss potential collaboration.

During Research Advisory Forum (RAF) held at Queensland University of Technology in Nov 2018, A/Prof Khalid Moinuddin presented various areas of conducted research and plans for future works. Our PhD student Rahul Wadhwani presented a three-minute

thesis on short range ember flux modelling. In the break-out session, we elaborately discussed emerging opportunity in physics-based simulation of grassfires with varying fuel moisture content and fuel weight/ height. The identification of threshold conditions for wind-driven propagation vs buoyancy-driven propagation as a function of fuel moisture content, fuel configuration, wind speed etc will be useful to refine rate of spread models. The session was attended by members of RFS NSW, CFA Victoria, QFES and other agencies.

A/Prof Khalid Moinuddin met Mr Brad Davies of RFS, NSW in Sydney during 6th International Fire Behavior & Fuels Conference in Apr 2019. Mr Davies showed some line scan data obtained during some real bushfire events. Victoria University and RFS, NSW are currently developing a data sharing agreement so that Victoria University can obtain the real fire propagation data. These scenarios will be modelled using Spark with default WRF and WRF function obtained using physics-based model. For each scenario, the comparison will be made between actual fire progression and that from two Spark simulations.

A/Prof Khalid Moinuddin, Dr Nazmul Khan and Dr Mahmood Rashid attended a field trip on 03 Apr 2019 organised by RFS NSW to be familiarised with fire bahviour analysis tools and techniques. A casy study of the mid-April 2018 Moorebank Ave that impacted Sydney's southern suburb was used. The field trip also included a visit to Sandy Point Fire Brigade.

CSIRO collaboration

A/Prof Khalid Moinuddin and Dr Nazmul Khan met Dr James Hilton of CSIRO Data61 at CSIRO Dockland, Melbourne office in Jan, 2019. Topics discussed were:

- Overview of Victoria University (VU) research areas – presented by Assoc Prof Moinuddin
- Overview and brief demonstration of Spark - presented by Dr Hilton
- Discussion on how the required utilisation can be developed
- Presentation of operational ember flux modelling at 6th International Fire Behaviour and Fuels Conference (Sydney, 2019).

A/Prof Moinuddin presented four areas of research: grassfire modelling, wind flow through forest canopies, short range ember flux modelling and surface to crown fire transition. Dr Hilton demonstrated the inclusion of "qualitative" ember flux submodel within SPARK. There are two areas of VU research which can be utilised within SPARK. These are (a) inclusion of statistical ember flux distribution with a view to assess house/infrastructure siting and design based on performance-based principle and (b) implement and test wind reduction factor (WRF) for various types of forest canopies. We have chosen SPARK as it is built on modular components.

Dr Mahmood Rashid joined our research group on 21 Feb 2019 as a Research Officer to assist utilization of our research (primarily WRF). Originally a Mechanical Engineer, Mahmood has a PhD in Computer Science from Griffith University, a year of postdoc experience in US and few years of teaching experience in Fiji. In Mar 2019, Mr Amila Wickramasinghe (a Chemical Engineer) joined as a PhD student for research into inclusion of ember flux in AS 3959 [3]. Both of them undertook a number of training modules to learn SPARK and identify ways to implement VU research in the system. They have been given access to SPARK so that they can log on from VU computers. It will be a collaborative process to test and implements improvements or modifications that need to be made.

CONTINUING WORKING RELATIONSHIPS WITH RESEARCHERS IN FRANCE/ LEBANON

France is subject to bushfires that are often in the vicinity in built infrastructure. This has given rise to the establishments a number of research groups that work on physics-based modelling of fires. During Prof Graham Thorpe 2014 visit, a collaboration was forged with Aix-Marseille University. As continuation Prof Morvan delivered a series of seminars to members of the project team at Victoria University in 2016 and a PhD student of him spent three-months with us in 2017. The PhD student was studying the space needed downstream of a canopy to recover an atmospheric wind profile using their physics-based model in FIRESTAR. Prof Morvan's long time associate Prof Gilbert Accary from Lebanese University will visit us later this year and will attend MODSIM 2019 conference in Canberra.

CURRENT TEAM MEMBERS

RESEARCH TEAM

Assoc Prof Khalid Moinuddin, Victoria University

Dr Duncan Sutherland, UNSW, Canberra/ Victoria University

Dr Nazmul Khan, Victoria University

Prof Andrew Ooi, University of Melbourne

Dr Jimmy Philip, University of Melbourne

Dr Mahmood Rashid, Victoria University

PHD STUDENTS

Mrs Jasmine Innocent, Victoria University

Mr Niteesh George, University of Melbourne

Mr Gavin Maund, Victoria University

Mr Amila Wickramasinghe, Victoria University

Dr Mahfuz Sarwar, Victoria University (completed)

Dr Michael MacDonald, University of Melbourne (completed)

Mr Rahul Wadhwani, Victoria University (thesis submitted)

Masters by Research students

Ms Sesa Singha Roy, Victoria University (thesis submitted)

END USERS

Dr Simon Heemstra, Manager Community Planning, NSW Rural Fire Service

Dr Stuart Matthews, Senior Project Officer, NSW Rural Fire Service

Mr Andrew Stark, Deputy Chief Officer, Country Fire Service South Australia

Mr Lawrence McCoy, Senior Fire Behaviour Analyst, NSW Rural Fire Service

Mr Brad Davies, Senior Fire Behaviour Analyst, NSW Rural Fire Service

Mr Chris Wyborn, Senior Technical Officer, Fire Protection Association of Australia

Mr Mike Wouters, Senior Fire Ecologist, DENS, South Australia

Mr Jackson Parker, Senior Environmental Officer, DEFS, WA

Mr Paul Fletcher, Assistant Chief Fire Officer, SAMFS

Mr Andrew Sturgess, Fire behaviour analyst, Queensland Fire and Emergency Services

Mr Brian Levine, Fire Management Officer, Parks and Conservation Service, ACT

Mr Adam Leavesley, Fire Management Officer, Parks and Conservation Service, ACT

REFERENCES

[1]   A. L. Sullivan, "Wildland surface fire spread modelling, 1990–2007. 2: Empirical and quasi-empirical models," *International Journal of Wildland Fire*, vol. 18, no. 4, pp. 369-386, 2009.

[2]   M. G. Cruz and M. E. Alexander, "Uncertainty associated with model predictions of surface and crown fire rates of spread," *Environmental Modelling & Software*, vol. 47, pp. 16-28, 2013.

[3]   "AS 3959 : Construction of Buildings in Bushfire-prone Areas : Standards Australia : Sydney," 3rd Edition 2009.

[4]   B. Nebenführ and L. Davidson, "Large-eddy simulation study of thermally stratified canopy flow," *Boundary-layer meteorology*, vol. 156, no. 2, pp. 253-276, 2015.

[5]   D. Sutherland, K. Moinuddin, and A. Ooi, "Large-eddy simulation of neutral atmospheric surface layer flow over heterogeneous tree canopies," in *Research Forum 2017: proceedings from the Research Forum at the Bushfire and Natural Hazards CRC and AFAC Conference, Sydney, Australia, 4–6 September 2017*, 2017, pp. 184-199: Bushfire and Natural Hazards CRC.

[6]   K. B. McGrattan, B. Klein, S. Hostikka, and J. Floyd, *Fire Dynamics Simulator Users Guide* (National Institute of Standards and Technology, U.S. Department of Commerce, Gaithersburg, MD, no. NIST Special Publication 1019-5). January 2008.

[7]   A. Dyer, "A review of flux-profile relationships," *Boundary-Layer Meteorology*, vol. 7, no. 3, pp. 363-372, 1974.

[8]   R. H. Shaw and U. Schumann, "Large-eddy simulation of turbulent flow above and within a forest," *Boundary-Layer Meteorology*, vol. 61, no. 1-2, pp. 47-64, 1992.

[9]   E. Inoue, "On the Turbulent Structure of Airflow within," *Journal of the Meteorological Society of Japan. Ser. II*, vol. 41, no. 6, pp. 317-326, 1963.

[10]   I. N. Harman and J. J. Finnigan, "A simple unified theory for flow in the canopy and roughness sublayer," *Boundary-layer meteorology*, vol. 123, no. 2, pp. 339-363, 2007.

[11]   W. J. Massman, J. Forthofer, and M. A. Finney, "An improved canopy wind model for predicting wind adjustment factors and wildland fire behavior," *Canadian Journal of Forest Research*, vol. 47, no. 5, pp. 594-603, 2017.

[12]   K. Moon, T. Duff, and K. Tolhurst, "Sub-canopy forest winds: understanding wind profiles for fire behaviour simulation," *Fire Safety Journal*, 2016.

[13]   T. E. R. Network and A. N. Uinversity. (2019). *Landscape Data Visualiser*.

[14]   K. A. M. Moinuddin, D. Sutherland, and R. Mell, "Simulation study of grass fire using a physics-based model: striving towards numerical rigour and the effect of grass height on the rate-of-spread," *International Journal of Wildland Fire*, vol. 27, no. 12, pp. 800-814, 2018.

[15]   N. Cheney, J. Gould, and W. Catchpole, "The influence of fuel, weather and fire shape variables on fire-spread in grasslands," *International Journal of Wildland Fire*, vol. 3, no. 1, pp. 31-44, 1993.

[16]   I. Noble, A. Gill, and G. Bary, "McArthur's fire-danger meters expressed as equations," *Australian Journal of Ecology*, vol. 5, no. 2, pp. 201-203, 1980.

[17]   N. Cheney, J. Gould, and W. R. Catchpole, "Prediction of fire spread in grasslands," *International Journal of Wildland Fire*, vol. 8, no. 1, pp. 1-13, 1998.

[18]   J. Dold and A. Zinoviev, "Fire eruption through intensity and spread rate interaction mediated by flow attachment," *Combustion Theory and Modelling*, vol. 13, no. 5, pp. 763-793, 2009.

[19]   D. Morvan and N. Frangieh, "Wildland fires behaviour: wind effect versus Byram's convective number and consequences upon the regime of propagation," *International Journal of Wildland Fire*, vol. 27, no. 9, pp. 636-641, 2018.

[20]   W. Mell, M. A. Jenkins, J. Gould, and P. Cheney, "A physics-based approach to modelling grassland fires," *International Journal of Wildland Fire*, vol. 16, no. 1, pp. 1-22, 2007.

[21]   N. Jarrin, S. Benhamadouche, D. Laurence, and R. Prosser, "A synthetic-eddy-method for generating inflow conditions for large-eddy simulations," *International Journal of Heat and Fluid Flow*, vol. 27, no. 4, pp. 585-593, 2006.

[22]   J. Sharples, "Risk Implications of Dynamic Fire Propagation," 2017.

[23]   J.-L. Dupuy and J. Maréchal, "Slope effect on laboratory fire spread: contribution of radiation and convection to fuel bed preheating," *International Journal of Wildland Fire*, vol. 20, no. 2, pp. 289-307, 2011.

[24]   R. C. Rothermel, "A mathematical model for predicting fire spread in wildland fuels," 1972.

[25]   M. Vonlanthen, J. Allegrini, and J. Carmeliet, "Assessment of a one-way nesting procedure for obstacle resolved large eddy simulation of the ABL," *Computers & Fluids*, vol. 140, pp. 136-147, 2016.

[26]   H. Davies, "A laterul boundary formulation for multi-level prediction models," *Quarterly Journal of the Royal Meteorological Society*, vol. 102, no. 432, pp. 405-418, 1976.

[27]   R. Linn, J. Canfield, P. Cunningham, C. Edminster, J.-L. Dupuy, and F. Pimont, "Using periodic line fires to gain a new perspective on multi-dimensional aspects of forward fire spread," *Agricultural and forest meteorology*, vol. 157, pp. 60-76, 2012.

[28]   M. G. Cruz, J. S. Gould, M. E. Alexander, A. L. Sullivan, W. L. McCaw, and S. Mathews, *Guide to Rate of Fire Spread Models for Australian Vegetation*. CSIRO Land and Water Flagship, Canberra, ACT and AFAC, Melbourne, VIC, 2015.

[29]   C. S. Tarifa, P. P. del Notario, and F. G. Moreno, "On the flight paths and lifetimes of burning particles of wood," in *Symposium (International) on Combustion*, 1965, vol. 10, no. 1, pp. 1021-1037: Elsevier.

[30]   A. Filkov *et al.*, "Investigation of firebrand production during prescribed fires conducted in a pine forest," *Proceedings of the Combustion Institute*, vol. 36, no. 2, pp. 3263-3270, 2017.

[31]   S. L. Manzello and S. Suzuki, "Experimentally simulating wind driven firebrand showers in Wildland-Urban Interface (WUI) fires: overview of the NIST firebrand generator (NIST dragon) technology," *Procedia Engineering*, vol. 62, pp. 91-102, 2013.

[32]   Y. Li and D. Drysdale, "Measurement of the ignition temperature of wood," *Fire Safety Science*, vol. 1, pp. 380-385, 1992.

[33]   J. S. Gould, W. McCaw, N. Cheney, P. Ellis, I. Knight, and A. Sullivan, *Project Vesta: fire in dry eucalypt forest: fuel structure, fuel dynamics and fire behaviour*. Csiro Publishing, 2008.

[34]   N. Khan, D. Sutherland, R. Wadhwani, and K. Moinuddin, "Physics-based simulation of heat load on structures for improving construction standards for bushfire prone areas," *Frontiers in Mechanical Enigineering*, p. (submitted), 2019.

[35]   K. Moinuddin and D. Sutherland, "Modelling of tree fires and fires transitioning from the forest floor to the canopy with a physics-based model," *Mathematics and Computers in Simulation*, vol. (submitted), 2019.

[36]   D. Sutherland, J. Philip, A. Ooi, and K. A. M. Moinuddin, "Large Eddy Simulation of Flow Over Streamwise Heterogeneous Canopies: Quadrant Analysis," in *21st Australasian Fluid Mechanics Conference*, Adelaide, Australia, 2018.

[37]   S. S. Roy, D. Sutherland, N. Khan, and K. A. M. Moinuddin, "A comparative study of wind fields generated by different inlet parameters and their effects on fire spread in Fire Dynamics Simulator," in *21st Australian Fluid Mechanics Conference*, Adelaide, Australia, 2018.

[38]   D. Sutherland, R. Wadhwani, J. Philip, A. Ooi, and K. Moinuddin, "Simulations of the effect of canopy density profile on sub-canopy wind speed profiles," 2018.

[39]   R. Wadhwani, D. Sutherland, and K. Moinuddin, "Simulated transport of short-range embers in an idealised bushfire," in *Proceedings for the 6th International Fire Behavior and Fuels Conference*, 2019: International Association of Wildland Fire.